Physica 21D (1986) 267–295
North-Holland, Amsterdam

# BOUNDARY CIRCLES FOR AREA-PRESERVING MAPS

J.M. GREENE*, R.S. MACKAY and J. STARK
*Mathematics Institute, University of Warwick, Coventry, UK*

Received 22 February 1986

We report on numerical observations of various properties of "boundary circles" for area-preserving maps. We find that the continued fraction expansion of their rotation number generally has a special form. We describe how their rotation number changes as parameters are varied. We observe a statistically self-similar structure in the neighbourhood of boundary circles, which is probably relevant to the long time tails of the decay of correlations in the irregular components.

## 1. Introduction

The phase space of a non-integrable Hamiltonian system is typically made up of a complicated mixture of regular and irregular regions. In the regular components the motion is quasiperiodic on 'KAM' tori, while in an irregular component the motion appears to lack order and to typically cover the component densely. In this context attention has been focused on two main issues in recent years: firstly to see how the regular 'KAM' tori break up as a parameter is varied ([1–5], and references therein); and secondly to understand, at least in some statistical sense, the behaviour of orbits in the irregular components ([6–10], and references therein).

Much of the work on these topics has been done in the context of area-preserving maps. These are the simplest non-trivial examples of conservative systems and occur as Poincaré maps for Hamiltonian flows of two degrees of freedom.

In this paper we present some numerical data on boundary circles in area-preserving maps, that is invariant circles which are isolated on at least one side from circles of 'the same class'. Such circles are thus on the boundary of an irregular component of phase space. They are believed to be relevant to both of the problems mentioned above. On the one hand they typically appear to be "critical", that is they can be destroyed by arbitrarily small perturbations of the map. On the other hand the structure near a boundary circle is important for the long time behavior of orbits in the irregular components. It seems that chaotic orbits can get 'stuck' near boundary circles for long periods of time, and this is offered as an explanation of the long time correlations observed [7, 8, 9, 11, 12].

In section 2 we give a precise definition of a boundary circle and give some basic properties, then in section 3 we describe a heuristic algorithm for finding boundary circles based on the residue criterion [1]. This generates the continued fraction expansion of the rotation number directly. We then present numerical evidence that the continued fraction is not arbitrary but is restricted to a particular subset, and we give statistics for the distribution of the terms. In this paper we present a short heuristic explanation. We hope to give a more satisfactory explanation in terms of renormalisation theory in a future paper. In section 5 we go on to discuss the behaviour of a progression of boundary circles as a parameter is varied. In section 6 we examine how Mather's $\Delta W$ [13] scales in the neighbourhood of a boundary circle,

*GA Technologies, San Diego, CA 92138, USA.

and remark on the relevance of the approximate self-similarity that we find to predictions about the decay of correlations in the irregular components. We also observe coordinate scaling in the neighbourhood of the dominant symmetry points on a boundary circle with approximately universal scaling exponents. Finally we study the linear stability of nearby periodic orbits, which suggests the existence of a Cantor set for the renormalisation mapping which governs the behaviour of boundary circles.

## 2. Boundary circles

### 2.1. *Definitions*

*Definition* 2.1. Let $M$ be an orientable surface and $\Gamma_1, \Gamma_2 \subset M$ be two embedded circles in $M$. Then $\Gamma_1, \Gamma_2$ are of the *same class* if there exists an annulus $A \simeq \mathbb{T}^1 \times [0,1]$ in $M$ s.t. $\Gamma_1$ and $\Gamma_2$ are the two components of the boundary of $A$ in $M$ (see fig. 1).

*Definition* 2.2. Let $T: M \to M$ be an area-preserving map of an orientable surface. Then a *boundary circle* (for $T$) is a circle invariant under $T$ which is isolated on at least one side from invariant circles of the same class, that is there exists a one-sided neighbourhood $\Omega$ of $\Gamma$ through which pass no invariant circles of the same class (fig. 2). We shall call this side of the circle the *stochastic side*. If a boundary circle is isolated on both sides we call it an *isolated circle*.

*Definition* 2.3. Recall (e.g. [14, 15]) that if $f: \mathbb{T}^1 \to \mathbb{T}^1$ is a homeomorphism of the circle, and $F$ is a lift of $f$, one can define the *rotation number* $\rho(F)$ of $F$ by

$$\rho(F) = \lim_{n \to \pm\infty} \frac{F^n(x) - x}{n}.$$

Then $\rho(F) \pmod 1$ is independent, up to a sign change, of the choice of lift and we call it the rotation number of $f$. If $\Gamma$ is an invariant circle for an area-preserving map $T$, then $T$ induces a

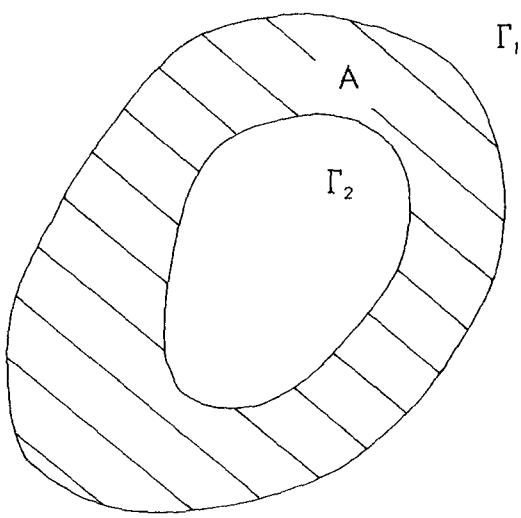


Fig. 1. Two circles $\Gamma_1$ and $\Gamma_2$ of the same class.

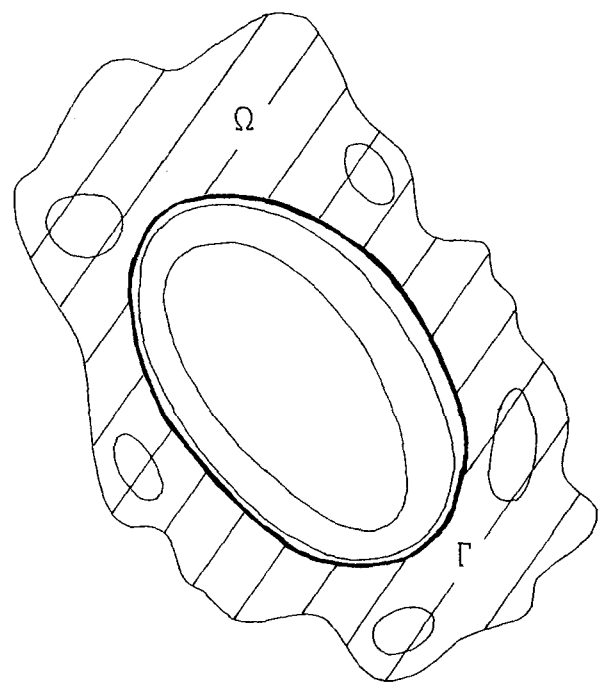


Fig. 2. A boundary circle $\Gamma$.

homeomorphism on $\Gamma$. We will refer to the rotation number of this homeomorphism as the *rotation number* of $\Gamma$.

*Definition* 2.4. A *critical circle* $\Gamma$ is an invariant circle which can be "destroyed" by an arbitrarily small smooth perturbation. More precisely there are arbitrarily small perturbations $T'$ of $T$ for which there is a neighbourhood of $\Gamma$ which contains no circle invariant under $T'$ of the same class and rotation number as $\Gamma$. For definiteness take the smoothness class to be analytic or $C^\infty$.

Numerical observation suggests that all boundary circles are critical, but this remains an open problem.

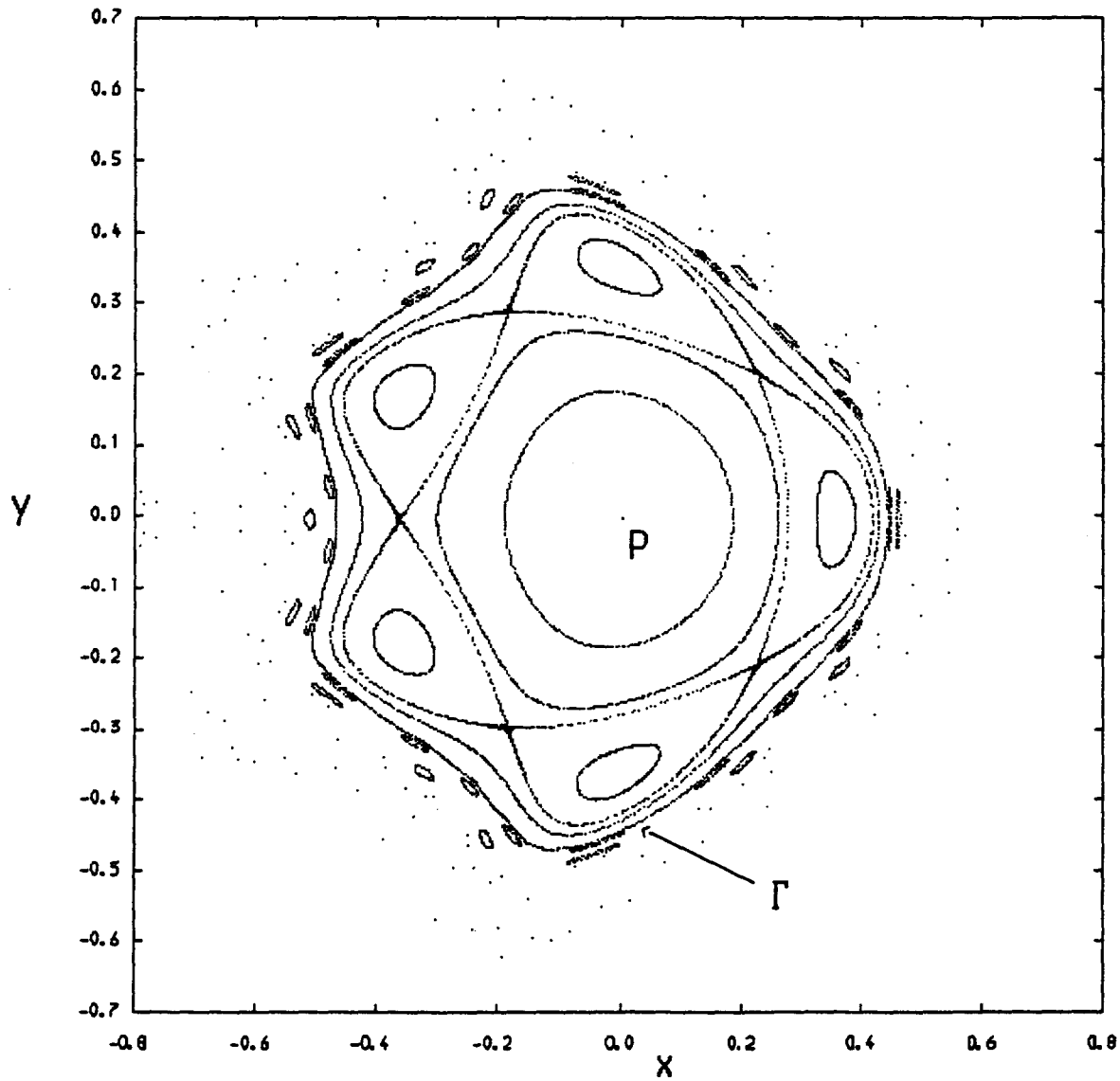


Fig. 3. The outermost circle $\Gamma$ of an elliptic fixed point $P$ for the quadratic map (4.2) at $c = 0.24$. $\Gamma$ crosses the positive $x$ axis $\{y = 0\}$ at $x = 0.440412907000782283\ldots$.

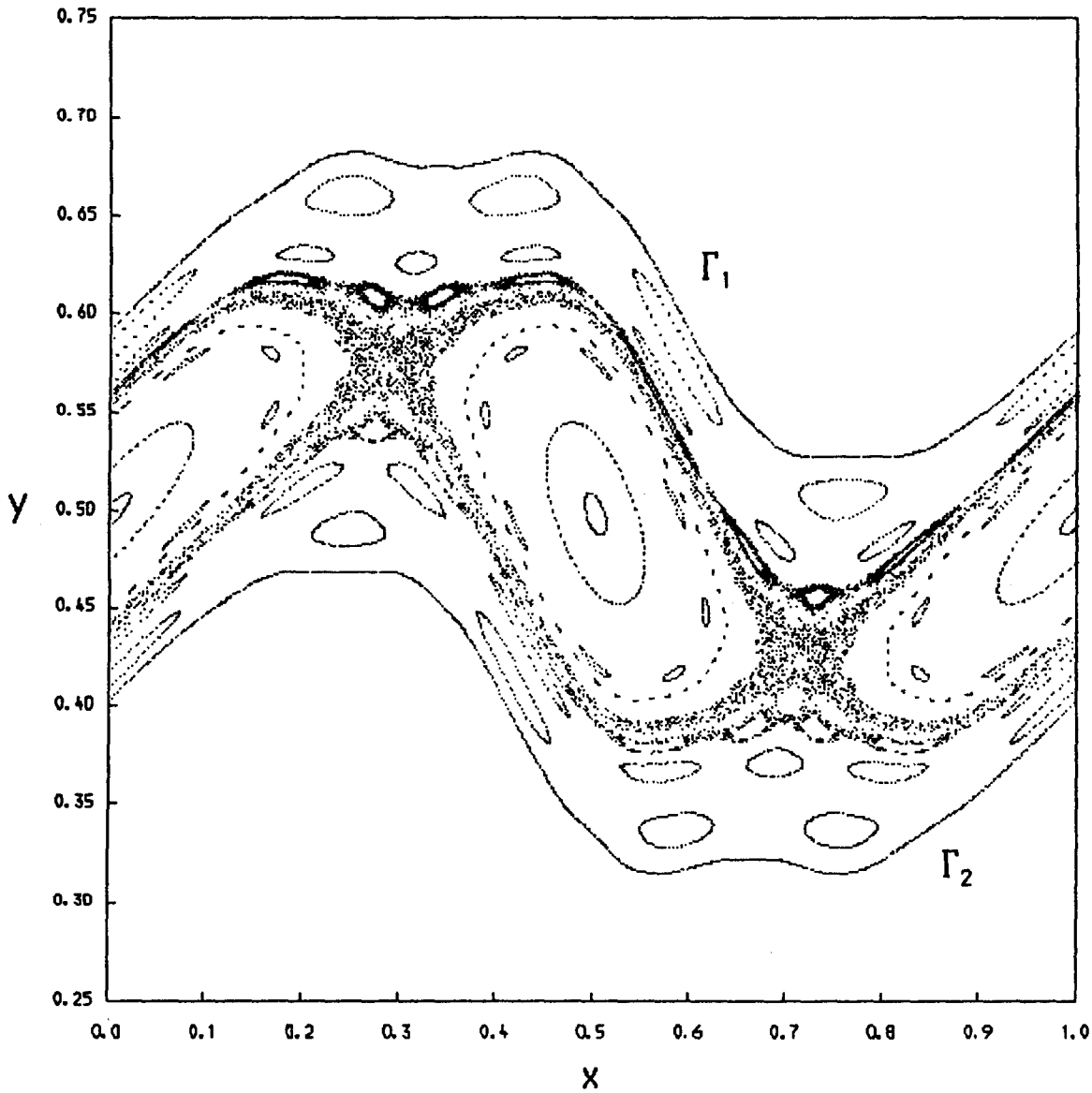


Fig. 4. Boundary circles $\Gamma_1$ and $\Gamma_2$ of the Birkhoff zone of instability around the period two island chain for the standard map (4.1) at $k = 0.97$. We have shown 10,000 points on the orbit of a point in an irregular component; note that in this time the orbit has by no means explored the full area accessible to it. $\Gamma_1$ and $\Gamma_2$ cross $\{x = 0\}$ at $y = 0.59492459\ldots$ and $0.40507541\ldots$, respectively.

Note that if $\Gamma$ is a boundary circle, then there may be arbitrarily close circles in $\Omega$ which are invariant under some power of $T$, but of a different class from $\Gamma$ (island chains). Many of these will be boundary circles themselves under the appropriate power of $T$.

*Examples* 2.5. a) outermost circle around an elliptic fixed point (fig. 3). b) boundaries of a Birkhoff Zone of Instability (fig. 4).

### 2.2. *Twist maps and rotational invariant circles*

*Definition* 2.6. Recall that an area-preserving diffeomorphism $T$ of an annulus $A = \mathbb{T}^1 \times [0,1]$ (or a

cylinder $\mathbb{T}^1 \times \mathbb{R}$) is said to be a *twist map* if $\forall (x, y) \in A$:

$$\partial x'/\partial y > 0, \quad \text{where } (x', y') = T(xy).$$

For such a map a *rotational invariant circle* (r.i.c.) is an invariant circle which is homotopically non-trivial, i.e. intuitively it winds once round $A$. By Birkhoff's Theorem (e.g. [Herman, [16] ch. 1]) all such circles are graphs of Lipschitz functions $\eta : \mathbb{T}^1 \to [0,1]$.

Twist is a common property and twist maps are by far the most studied class of area-preserving maps. We shall thus mainly be interested in boundary circles which are rotational invariant circles for a twist map of the annulus. Note that even though a map may not have twist globally we can often find an annulus locally on which the map is a twist map, and in particular given an invariant circle $\Gamma$, in many cases we can find an annulus $A$ on which $T$ is a twist map and for which $\Gamma$ is rotational.

Note that boundary circles do indeed occur quite frequently. For a twist map the set of rotational invariant circles is closed [Herman [16], ch. 1, section 5.5]. Thus if there is at least one rotational invariant circle and there is at least one point through which no rotational invariant circle passes (so the map is non-integrable) then there is at least one boundary rotational invariant circle. Typically if there is one, there are infinitely many.

### 2.3. *Rotation numbers*

A natural generalisation of 2.2 to twist maps of the annulus (or cylinder) is:

*Definition* 2.7. Let $T^* : \mathbb{R} \times [0,1] \to \mathbb{R} \times [0,1]$ be a lift of an area-preserving map $T$ of the annulus $\mathbb{T}^1 \times [0,1]$, and let $\pi : \mathbb{R} \times [0,1] \to \mathbb{R}$ be the projection $\pi(x, y) = x$. If for a given $x \in \mathbb{R} \times [0,1]$ the limit

$$\rho(x) = \lim_{n \to \pm\infty} \frac{\pi(T^{*n}(x)) - \pi(x)}{n}$$

exists, then $\rho(x) \pmod 1$ is independent of the choice of lift of $T$ and is called the *rotation number* of $x$ for $T$.

Note that since rotational invariant circles are graphs of Lipschitz functions every orbit on such a circle has a rotation number. If we choose compatible orientations for the two lifts involved this rotation number is clearly equal to the rotation number of the circle given by 2.2.

*Definition* 2.8. Let $[\omega_1, \omega_2]$, $\omega_1 < \omega_2$, be an interval such that there exists a rotational invariant circle with rotation number in $[\omega_1, \omega_2]$. Define

$$\omega_{\min}[\omega_1, \omega_2] = \min\{\omega \in [\omega_1, \omega_2]: \text{ there exists a rotational invariant circle of rotation number } \omega\}.$$

The minimum exists since the set of rotation numbers of rotational invariant circles is closed ([Herman, [16], ch. 1]). For completeness if there is no rotational invariant circle with rotation number in $[\omega_1, \omega_2]$ we define $\omega_{\min}[\omega_1, \omega_2] = \omega_2$. Finally we define $\omega_{\max}[\omega_1, \omega_2]$ similarly.

Note that if there is no rotational invariant circle of rotation number $\omega_1$, but there is some circle with rotation number in $[\omega_1, \omega_2]$, then the circle of rotation number $\omega_{\min}[\omega_1, \omega_2]$ will be a boundary circle.

The behaviour of an invariant circle depends crucially on the number theoretic properties of its rotation number $\omega$, and in particular on how well $\omega$ can be approximated by rationals. Generically invariant circles have irrational rotation number [17], and in some sense (made precise below) the more irrational the rotation number is, the more robust the circle is. For this reason it turns out to be fruitful to study the *continued fraction expansion* of $\omega$:

$$\omega = a_0 + \cfrac{1}{a_1 + \cfrac{1}{a_2 + \cfrac{1}{a_3 \cdots}}}$$

If $\omega$ is rational this expansion terminates, otherwise if $\omega$ is irrational it has an infinite number of terms. In our case since we always consider $\omega \in [0,1)$ we have $a_0 = 0$ and so for notational convenience we will write $\omega = [a_1, a_2, a_3, \ldots]$. In general we are only interested in the asymptotic behaviour of the terms $a_i$ as $i \to \infty$. Thus by the *tail* of the continued fraction expansion we mean the $a_i$ for all $i > N$, for some $N \in \mathbb{N}$. The *head* of the continued fraction is then the terms $a_1, \ldots, a_N$. To denote a tail which is constant or periodic we will use the notation $(b_1, \ldots, b_n)_\infty$ to mean $b_1, \ldots, b_n, \ldots, b_n, b_1, \ldots, b_n, \ldots$. Thus $1/\gamma = [(1)_\infty] = [1,1,1,1,\ldots] = (\sqrt{5}-1)/2$ is the reciprocal of the golden mean.

Given $\omega = [a_1, a_2, a_3, \ldots]$ irrational, define the *convergents* $p_n/q_n$ of $\omega$ by

$$p_n/q_n = [a_1, a_2, \ldots, a_n] = \cfrac{1}{a_1 + \cfrac{1}{a_2 + \cfrac{1}{a_3 \cdots}}} \cdots + \frac{1}{a_n}.$$

These are the best rational approximants to $\omega$ in the sense of diophantine approximation, i.e. $|\omega - p/q| > |\omega - p_n/q_n|$ for all other $p/q$ with $q < q_{n+1}$ [18].

Note that successive convergents to $\omega \in \mathbb{R} \setminus \mathbb{Q}$ approximate $\omega$ from opposite sides, i.e. if $p_n/q_n > \omega$ then $p_{n+1}/q_{n+1} < \omega$, and vice versa. For boundary circles we expect different behaviour on the two sides of the circle, thus it is useful to distinguish between alternate convergents:

*Definition* 2.9. Let $\omega \in \mathbb{R} \setminus \mathbb{Q}$ be the rotation number of a rotational boundary circle $\Gamma$. We call a convergent $p_n/q_n = [a_1, a_2, \ldots, a_n]$ to $\omega$ an *outer convergent* if the periodic orbits with rotation number $p_n/q_n$ lie on the isolated side of the circle. We then call $a_n$ an *outer coefficient* of the continued fraction expansion of $\omega$. Similarly $p_n/q_n$ is an *inner convergent* if the corresponding periodic orbits lie on the regular side of the circle, and the corresponding term in the continued fraction is then called an *inner coefficient*.

If $\Gamma$ is a rotational boundary circle of rotation number $\omega = [a_1, a_2, a_3, \ldots]$, then either the isolated side of the circle corresponds to rotation numbers less than $\omega$, or greater than $\omega$. In the first case the outer convergents are less than $\omega$ and the outer coefficients are the even terms in $[a_1, a_2, a_3, \ldots]$, i.e. we can write $\omega = [b_1, c_1, b_2, c_2, b_3, c_3, \ldots]$ where the $b_i$ are the inner coefficients and the $c_i$ are the outer. Similarly if the isolated side corresponds to rotation numbers greater than $\omega$, then the outer coefficients are the odd terms in the continued fraction.

### 2.4. *Noble circles*

The most irrational numbers (in the above sense) are the so-called *noble* numbers, whose continued fraction expansion has tail $[(1)_\infty]$ (i.e. is of the form $[a_1, \ldots, a_n, (1)_\infty]$). A great deal is known about the nearby structure around a critical invariant circle of noble rotation number [3, 4, 5, 19]. It appears to be asymptotically self-similar in the neighbourhood of certain points on the circle, with a universal form (see sections 6.1 and 6.2). The breakup of such circles is governed by a universal one-parameter family (see section 5.2). In particular, critical noble circles always seem to be isolated and it is conjectured that all isolated circles have noble rotation number (and are critical). To some extent the data we present in sections 4 and 5 supports this conjecture.

We do not, however, expect all boundary circles to be noble; in fact we expect this to be very rare. Consider a one parameter family $T_\mu$ of area-preserving maps, and let $\omega_{\min}(\mu)$ be the smallest rotation number of the invariant circles for $T_\mu$ of a given class in some given interval $(\omega_1, \omega_2)$. Then the set of parameter values for which $\omega_{\min}(\mu)$ is noble will typically have measure zero. This is because given a noble number (or indeed any number), existence of an isolated invariant circle of a given class with that rotation number appears

to be a codimension one property. It thus only happens for isolated values of the parameter in typical one parameter families. The set of noble numbers is countable and hence has measure zero. Thus we conclude that noble boundary circles are rare.

### 2.5. *Smoothness*

In general we do not expect the conjugacy to a uniform rotation (if it even exists) for a boundary circle to be differentiable many times. This is because given a circle $\Gamma$ with Diophantine rotation number (and our data from section 4 suggests that this applies to most boundary circles) if it has local twist and sufficiently smooth conjugacy to rotation one can change coordinates locally to make the map look arbitrarily close to integrable [Mather, private communication]. Then the Moser Twist Theorem [20] gives the existence of other invariant circles of the same class arbitrarily close on both sides of $\Gamma$, and thus $\Gamma$ cannot be a boundary circle.

## 3. Locating boundary circles

### 3.1. *Introduction*

In this section we discuss one way to find rotational boundary circles for an area-preserving twist map numerically, and how to determine their rotation number. As we remarked in the previous section a rotational invariant circle with rotation number $\omega_{\min}[\omega_1, \omega_2]$ for some suitable rotation interval $[\omega_1, \omega_2]$ is a boundary circle. Conversely given a rotational boundary circle of rotation number $\omega$ there exists an interval $[\omega_1, \omega_2]$ with $\omega_1 < \omega_2$ such that either $\omega = \omega_{\min}[\omega_1, \omega_2]$ or $\omega = \omega_{\max}[\omega_1, \omega_2]$. In particular we can find rationals $p_0/q_0, p_1/q_1$ s.t. $p_1q_0 - p_0q_1 = 1$ and either $\omega = \omega_{\min}[p_0/q_0, p_1/q_1]$ or $\omega = \omega_{\max}[p_0/q_0, p_1/q_1]$. Without loss of generality it is enough to consider the first case only. We thus present an algorithm for finding $\omega_{\min}[p_0/q_0, p_1/q_1]$, based on the one hand on the residue criterion (section 3.3) and on the other on the following properties of pairs of rationals satisfying $p_1q_0 - p_0q_1 = \pm 1$.

### 3.2. *Neighbouring rationals*

*Definition* 3.1. We say rationals $p_0/q_0$ and $p_1/q_1$ are *neighbouring rationals* if they satisfy $p_1q_0 - p_0q_1 = \pm 1$. This is equivalent to $p_0/q_0$ and $p_1/q_1$ being adjacent terms in some Farey sequence [Hardy and Wright [18] ch. 3]. In terms of continued fractions it means that the expansions of $p_0/q_0$ and $p_1/q_1$ are of the form $[a_1, a_2, \ldots, a_n]$ and $[a_1, a_2, \ldots, a_n, m]$ for some $m \in \mathbb{N}$. If $p_0/q_0$ and $p_1/q_1$ are neighbouring define their *mediant* to be $p_2/q_2 = (p_1 + p_0)/(q_1 + q_0)$. This is then neighbouring to both $p_0/q_0$ and $p_1/q_1$.

Note that if $\omega$ is irrational and has continued fraction expansion $\omega = [a_1, a_2, a_3, \ldots]$ and $p_n/q_n = [a_1, a_2, \ldots, a_n]$ is the $n$th convergent to $\omega$, then $p_n/q_n$ and $p_{n+1}/q_{n+1}$ are neighbouring rationals. Conversely we can generate the continued fraction expansion of $\omega$ via a sequence of neighbouring rationals: define $p_0 = 0$, $q_0 = 1$, $p_1 = 1$, $q_1 = 0$. Let $p_2 = p_0 + p_1$ and $q_2 = q_0 + q_1$. Then either $\omega \in [p_0/q_0, p_2/q_2]$ or $\omega \in [p_2/q_2, p_1/q_1]$. Choose whichever interval $\omega$ does lie in, and repeat recursively. At each stage we thus choose either a left interval or a right interval. Write down the sequence of L's and R's representing this, e.g. LRRLRRRLLRRL.... If we precede this sequence by an L and then write down the number of symbols (L or R) in each group of consecutive L's or R's we obtain precisely the continued fraction expansion of $\omega$, e.g. the above sequence gives $[2, 2, 1, 3, 2, 2, 1, \ldots]$. This is a consequence of the fact that the convergents $p_n/q_n$ satisfy the recurrence relations $p_{n+1} = a_{n+1}p_n + p_{n-1}$ and $q_{n+1} = a_{n+1}q_n + q_{n-1}$. Note that we can apply the above procedure with $p_0/q_0, p_1/q_1$ different from $0/1$ and $1/0$, in which case to obtain the complete expansion for $\omega$, we have to combine the first term of the sequence obtained from counting L's and

R's in an appropriate manner with the continued fraction expansions of $p_0/q_0$ and $p_1/q_1$. Also note that the rationals at which one changes from L to R or vice versa are precisely the convergents of $\omega$. The others are called *intermediate* fractions.

3.3. *Residue criterion* [1]

This is an empirical method for determining the existence or non-existence of an invariant circle from the linear stability of nearby periodic orbits.

*Definition* 3.2. Given a periodic orbit of an area-preserving map $T$ of period $q$, its linear stability may be measured by its *residue* $R$ defined by

$$R = (2 - \mathrm{Tr}[DT^q])/4.$$

Given an area-preserving twist map $T$ of the annulus $A = \mathbb{T}^1 \times [0,1]$, let $\rho_0$ and $\rho_1$ be the rotation numbers of $T$ restricted to the two boundary circles $\mathbb{T}^1 \times \{0\}$ and $\mathbb{T}^1 \times \{1\}$ respectively. Then by the Poincaré–Birkhoff theorem [21, 22, 23, 24] for each rational $p/q \in [\rho_0, \rho_1]$, there exists at least one periodic orbit of rotation number $p/q$ with non-negative residue $R_{p/q}$. The residue criterion is then the conjecture that given $\omega \in [\rho_0, \rho_1]$, irrational, if $p_n/q_n$ are the convergents of $\omega$ one of the following occurs:

*Criterion* 3.3.

1) $R_{p_n/q_n} \to 0$ as $n \to \infty$ and there exists a smooth rotational invariant circle of rotation number $\omega$.

2) $R_{p_n/q_n} \to \infty$ as $n \to \infty$ and there exists no rotational invariant circle of rotation number $\omega$.

3) neither and there exists a critical rotational invariant circle of rotation number $\omega$.

For our purposes this form of the criterion has two disadvantages. Firstly it applies only to one rotation number at a time, whilst we need to determine non-existence of invariant circles for a whole interval of rotation numbers. Secondly, it is difficult for a computer to determine the limiting behaviour of a sequence.

However, Greene further remarked that in case 3) $R_{p_n/q_n} \to$ some value $R^* \simeq 0.2500\ldots$ for all noble rotation numbers $\omega$. Together with the assumption that the most robust circles are those with noble rotation number (section 2.4) we obtain the following criterion.

*Criterion* 3.4. Given two neighbouring rationals $p/q$ and $p'/q'$ there are no rotational invariant circles of rotation number in $[p/q, p'/q']$ if the residues $R_{p/q}$ and $R_{p'/q'}$ are significantly larger than 0.25. If the residues are significantly smaller then some such circles do exist.

Using the renormalisation theory of noble circles, MacKay [4, 19] then suggests the following refinement which is particularly suitable for implementation on a digital computer. The idea is that if there are any circles with rotation number between $p/q$ and $p'/q', q' > q$ then there is likely to exist a circle with rotation number $(p + \gamma p')/(q + \gamma q')$ (where $\gamma = (\sqrt{5} + 1)/2$ is the golden mean). This is the "most important" noble between $p/q$ and $p'/q'$. Using an approximation to the stable manifold of the fixed point of the renormalisation operator one obtains [19]:

*Criterion* 3.5. Given two neighbouring rationals $p/q$ and $p'/q'$ with $q' > q$, evaluate the weighted geometric mean:

$$\log R^* = \frac{\log R_{p/q} + \gamma \log R_{p'/q'}}{\gamma^2}.$$

Then there are or are not rotational invariant circles of rotation number between $p/q$ and $p'/q'$ depending on whether $R^*$ is significantly less than or greater than 0.25.

Correction terms when $q'/q$ is far from $\gamma$ are available too, but we did not bother using them.

With both criteria 3.4 and 3.5 if the result is inconclusive because the residues are too close to 0.25 we can subdivide $[p/q, p'/q']$ and test each subinterval separately. Because the renormalisa-

tion is expanding in the unstable direction, subdividing the interval leads to increased sensitivity, and hence towards a definite result. The most natural way of doing this is to subdivide into $[p/q, p''/q'']$ and $[p''/q'', p'/q']$ where $p''/q''$ is the mediant of $p/q$ and $p'/q'$ and then repeat recursively until a definite result is obtained (or numerical precision is lost). This is precisely the way that we implemented the residue criterion in our numerical work, using criterion 3.5 above. We used mainly 0.2 and 0.3 as lower and upper significance levels for $R^*$. However our results seemed to be very insensitive to these choices, or indeed to the precise form of the residue criterion used.

### 3.4. *Algorithm for finding* $\omega_{\min}$

Our algorithm determines $\omega_{\min}[p_0/q_0, p_1/q_1]$ by repeatedly subdividing $[p_0/q_0, p_1/q_1]$ and always choosing the "left-most" interval still containing a rotational boundary circle. Thus:

1) Subdivide $[p_0/q_0, p_1/q_1]$ using $p_2/q_2$, the mediant of $p_0/q_0$ and $p_1/q_1$.

2) Apply residue criterion to $[p_0/q_0, p_2/q_2]$.

3) If there is a rotational invariant circle in this interval apply algorithm recursively to determine $\omega_{\min}[p_0/q_0, p_2/q_2]$. Then $\omega_{\min}[p_0/q_0, p_1/q_1] = \omega_{\min}[p_0/q_0, p_2/q_2]$.

4) If there is no rotational invariant circle in $[p_0/q_0, p_2/q_2]$ apply algorithm recursively to obtain $\omega_{\min}[p_2/q_2, p_1/q_1]$. Then $\omega_{\min}[p_0/q_0, p_1/q_1] = \omega_{\min}[p_2/q_2, p_1/q_1]$.

In this way we obtain a sequence of intervals converging to $\omega_{\min}[p_0/q_0, p_1/q_1]$. As we saw in section 3.2 this process can be used to generate the continued fraction expansion of $\omega_{\min}$ directly. We terminate the algorithm when the numerical errors involved in determining $R_{p/q}$ become too large. Note that the location in phase space of the boundary circle can be obtained, if required, as the limit of the periodic orbits whose rotation numbers are the mediants of the converging intervals. We have to find these orbits anyway in order to evaluate their residue.

*Remarks* 3.6. a) If we need to subdivide $[p_0/q_0, p_2/q_2]$ in applying the residue criterion, and decide that there is indeed a rotational invariant circle in this interval, we will already have calculated some of the residues needed to apply the algorithm to $[p_0/q_0, p_2/q_2]$. The algorithm can thus be made much more efficient by storing this data rather than recalculating it.

b) If there is in fact no rotational invariant circle in $[p_0/q_0, p_1/q_1]$ then the algorithm will show this (up to the approximations involved).

c) Many area-preserving maps $T$ are reversible, i.e. there is a *reversor* $S$ with $S^2 = \mathrm{Id}$ which conjugates $T$ to its inverse: $S \circ T \circ S^{-1} = T^{-1}$. The fixed points of a reversor form curves called *reflection* or *symmetry lines*. For such maps there are periodic points of all rotation numbers on each of the reflection lines. It is much more efficient to use these 'symmetric' periodic orbits in evaluating $R_{p/q}$. Finding such orbits involves only a one-dimensional search rather than the usual two-dimensional one. Furthermore to evaluate the residue of such an orbit we need only go half-way around the whole orbit [3, 4]. It turns out that usually there is a reflection line on which occur periodic points of all rotation numbers $p/q$ with a non-negative residue. Such reflection lines are called *dominant*.

## 4. Rotation numbers of boundary circles

### 4.1. *Numerical work*

Most of our numerical work was done with the standard map:

$$y' = y - (k/2\pi)\sin(2\pi x), \qquad x' = x + y', \tag{4.1}$$

for which $x = 0$ is a dominant reflection line when $k \geq 0$. We chose parameter values ranging from 0.75 to 0.97, and mainly considered the circles $\omega_{\min}[0/1, 1/2]$ and $\omega_{\min}[1/2, 1/1]$. Using double precision arithmetic (16 significant figures) we

considered periodic orbits of period up to 50000. This gave between 11 and 18 terms of the continued fraction expansion of the boundary circle. The statistics of our results seem to be independent of parameter, and circles obtained from other choices of neighbouring rationals seem to exhibit the same properties. Altogether we considered some 500 boundary circles.

To obtain longer orbits efficiently we also looked at the quadratic map

$$x' = -y + cx - (1-c)x^2,$$
$$y' = x - cx' + (1-c)x'^2. \tag{4.2}$$

This is the map studied by Hénon with a change of coordinates and $c = \cos\alpha$. In this form $\{y = 0, x > 0\}$ is a dominant reflection line. We searched for the boundary circle with minimum $\omega$, i.e. the boundary of orbits that run away to infinity. The much reproduced case $\cos\alpha = 0.24$ was studied, and the longest periodic orbit considered had period 2054107. The results obtained for the quadratic map confirmed those from the standard map. To the extent that the standard and quadratic maps are typical of area-preserving twist maps we would expect the following results to apply to such maps in general.

### 4.2. *The tail of the continued fraction*

After the initial few terms the continued fraction expansion of the rotation number of boundary circles has a very definite form. As expected there is a marked dichotomy between outer and inner coefficients. The outer coefficients are always either a 1 or 2, the inner ones range from 1 to 5. Thus for example the outermost circle for the quadratic map at $\cos\alpha = 0.24$ appears to have rotation number $[5,4,2,1,3,1,3,1,4,1,1,1,2,1,1,1,\ldots]$ (fig. 3). The approximate distribution of the terms in the continued fraction expansion of boundary circles is given in table I. This data is an average over 5–12 terms in the continued fraction expansion of some 400 circles. We took all terms for each circle except the first four and the last two before loss of significance. However the distribution remains very similar if we take a more restricted subset of these terms. The last column of table I gives the expected distribution with respect to the Gauss measure $\mu_n = \log_2[(n+1)^2/n(n+2)]$, i.e. the expected distribution if the rotation numbers of boundary circles were uniformly distributed. We see that the outer coefficient is always almost a 1, whilst the inner coefficients are definitely biased away from 1.

Table I
Distribution of terms of the tail of the continued fraction expansion of boundary circles

| | Outer | Inner | Gauss |
|---|---|---|---|
| 1 | 90% | 29% | 42% |
| 2 | 10% | 38% | 17% |
| 3 | – | 24% | 9% |
| 4 | – | 8% | 6% |
| 5 | – | 1% | 4% |
| 6 | – | – | 3% |
| Total | 1774 | 1673 | |

– indicates that no occurrences were observed in the sample
0% means less than 0.5%.

Successive inner and outer coefficients do not appear to be completely independent. In tables II and III we thus give the distributions of the various (inner, outer) and (outer, inner) combinations. We see for instance that an inner 1 is almost never followed by an outer 2, whilst larger inner coefficients are more likely to be followed by outer 2's

Table II
Distributions of (inner, outer) pairs of coefficients

| Inner \ Outer | 1 | 2 |
|---|---|---|
| 1 | 29% | 0% |
| 2 | 34% | 3% |
| 3 | 20% | 4% |
| 4 | 6% | 2% |
| 5 | 0% | 1% |

Total = 1774

– indicates that no occurrences were observed in the sample
0% means less than 0.5%.

Table III
Distributions of (outer, inner) pairs of coefficients

| Outer \ Inner | 1 | 2 | 3 | 4 | 5 |
|---|---|---|---|---|---|
| 1 | 26% | 33% | 22% | 8% | 1% |
| 2 | 3% | 5% | 2% | – | – |

Total = 1673

– indicates that no occurrences were observed in the sample
0% means less than 0.5%.

than one would expect. Note that since we can only calculate a finite number of terms in the continued fraction for each circle, the samples for tables II and III were slightly different. This is the reason why the row and column totals for tables II and III are not completely consistent with each other. Table II does not add up to 100% due to rounding off to the nearest one percent.

If we apply the renormalisation operator $N_{a_1}$ of [5] to a boundary circle of rotation number $\omega = [a_1, a_2, \ldots]$, it remains a boundary circle, though the rotation number changes to $[a_2, a_3, \ldots]$ and the inner and outer sides interchange. Our description of the tail of the continued fraction of the rotation numbers of boundary circles can thus be thought of as related to the $\omega$-limit set of the set of all maps under the sequence of renormalisation mappings determined by their boundary circles. Thus given a boundary circle of rotation number $\omega = [a_1, a_2, \ldots]$ let $\omega_n = [a_{n+1}, a_{n+2}, \ldots]$ be the rotation number after $n$ renormalisations. It is also useful to introduce a second "frequency":

$$\nu_n = [a_n, a_{n-1}, \ldots, a_1] = \cfrac{1}{a_n + \cfrac{1}{a_{n-1} + \cfrac{1}{a_{n-2} \cdots}}} \cdots + \cfrac{1}{a_1}$$

(see refs. 25, 26). In fact $\nu_n = q_{n-1}/q_n$. We call $\nu_n$ the "head frequency" and $\omega_n$ the "tail frequency". The renormalisation then acts as a simple shift $\sigma$ on the $a_i$:

$$\omega_n = [a_{n+1}, a_{n+2}, \ldots,] \to [a_{n+2}, a_{n+3}, \ldots,],$$
$$\nu_n = [a_n, a_{n-1}, \ldots, a_1] \to [a_{n+1}, a_n, \ldots, a_1].$$

Since we are considering the asymptotic behaviour of $\omega_n$ and $\nu_n$, we like to think of the $a_n$ as defined for all $n \in \mathbb{Z}$. Thus $\nu_n$ can take irrational values. Then if we let $\Omega$ be the sequence $\Omega = \{a_i : i \in \mathbb{Z}\}$, $\sigma$ acts on $\Omega$ by $[\sigma(\Omega)]_i = a_{i+1}$. Because $\sigma$ interchanges inner and outer sides, the $\omega$-limit set has a natural period two behaviour. It is thus preferable to work with $\sigma^2$ and consider only one half of the set, corresponding to either $a_n$ inner or $a_n$ outer. Fig. 5 thus shows a plot of the observed pairs $(\nu_n, \omega_n)$ for $a_n$ an outer convergent. A Cantor set structure is clearly apparent, corresponding to the absence of large $a_n$. The frequencies of tables I, II and III are then a result of a $\sigma^2$ invariant measure on this set. It is clear that some regions are visited much less often than others, and some not at all. It would be interesting to see whether they ever are visited, and the measure is just very sparse on them, or these combinations of terms never occur in the continued fraction for a boundary circle. Unfortunately finding boundary circles is computationally very intensive and we were unable to plot more points for fig. 5. A related question is whether there is indeed an upper bound for the inner and outer coefficients or whether arbitrarily large values are possible but just very rare. We conjecture that for a generic set of area-preserving twist maps, the coefficients are indeed bounded. Thus, for instance, our numerical data suggests that in the class of maps describing the neighbourhood of a boundary circle the presence of a circle with rotation number between $[a_1, \ldots, a_{n-2}, 1, 6]$ and $[a_1, \ldots, a_{n-2}, 1, 7]$ implies the existence of a circle between $[a_1, \ldots, a_{n-2} + 1]$ and $[a_1, \ldots, a_{n-2} + 2]$. This would mean that there were no sixes in the asymptotic continued fraction expansion of boundary circles.

On the other hand it is possible to construct area-preserving twist maps with rotational in-

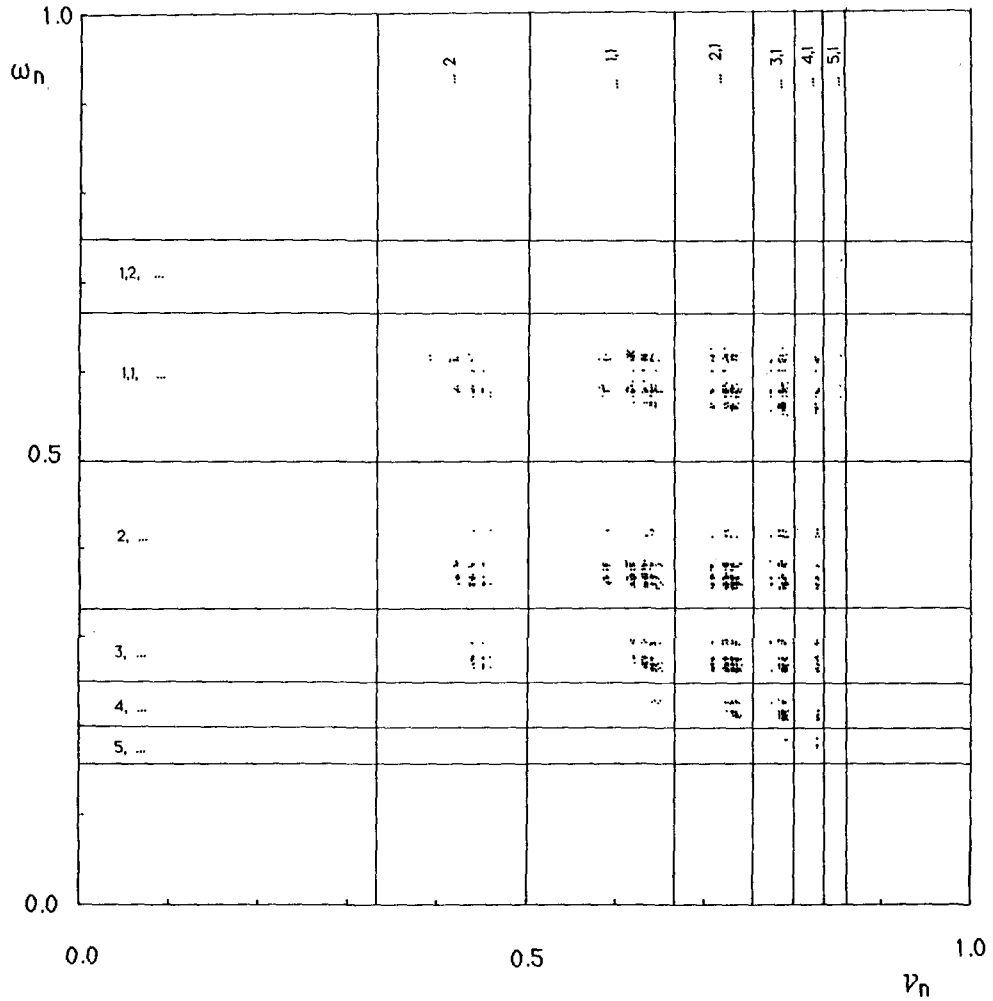


Fig. 5. $\nu_n$ against $\omega_n$ for the outer convergents of boundary circles. The cross at (0.618,0.618) marks the golden fixed point of the renormalisation, and the most significant terms in $\nu_n$ and $\omega_n$ are indicated.

variant circles of arbitrary rotation number [16]. It may be possible to modify this construction to give either an isolated or a boundary circle, and thus obtain boundary circles with arbitrary continued fractions for their rotation number, though we don't yet know how.

Finally, we remark that at least for the standard map, the above asymptotic behaviour is achieved very rapidly, normally within only one or two terms of the head determined by $p_0/q_0$ and $p_1/q_1$.

### 4.3. *Heuristic explanation*

We can give a heuristic explanation for these results as follows. Invariant circles are broken by having resonances too close to them. A suitable measure of closeness of a rational $p/q$ to a number $\omega$ is $q|q\omega - p|$. One thus expects isolated circles to have rotation numbers $\omega$ which maximize $\inf\{(q|q\omega - p|) : p/q \in \mathbb{Q} \cap J\}$ over some interval $J$ around $\omega$. This is equivalent to saying

that $\omega$ is noble. To see this note first that if $q_n \le q \le q_{n+1}$ (where $p_n/q_n$ is the $n$th convergent) then $q|q\omega - p| \ge q_n|q_n\omega - p_n|$. Thus in evaluating the above infimum we only need consider the convergents to $\omega$. For these we have the following formula:

$$\delta_n = q_n|q_n\omega - p_n|$$
$$= \frac{1}{\nu_n + \frac{1}{\omega_n}}$$
$$= \frac{1}{\frac{1}{\frac{1}{a_1} + \cdots + a_n} + a_{n+1} + \frac{1}{a_{n+2} + \frac{1}{a_{n+3}} \cdots}}$$

We then see that if there exists an $n$ s.t. $a_{n+1} \ge 3$, then $\delta_n < 1/3$. If no such $n$ exists but for some $n$ we have $a_{n+1} = 2$ then

$$\delta_n \le \cfrac{1}{1+\cfrac{2+\cfrac{1}{1+\cfrac{2+\cfrac{1}{1+\cfrac{1}{1+\cfrac{2+\cfrac{1}{2+\cdots}}}}}}}}$$
$$\le 1/(2\sqrt{3}) \simeq 0.288\ldots$$

On the other hand if $a_n = 1$ for all $n$ then $\delta_n \sim 1/(\gamma + 1/\gamma) \simeq 0.447\ldots$. Thus to maximize $\inf \delta_n$ we want the continued fraction of $\omega$ to have a tail $[\ldots(1)_\infty]$. This is precisely the condition for $\omega$ to be a noble and is the reason why one expects noble invariant circles to be the most robust.

For boundary circles one would expect $\omega$ to maximize the same expression, but now only over a one-sided neighbourhood $J$ of $\omega$. On the other side we would allow rational resonances to approach $\omega$ as closely as they like. An argument similar to the above then suggests that the tail of the continued fraction expansion of $\omega$ will have outer coefficients 1 and inner coefficients 'large'. This agrees roughly speaking with our observations, except that we occasionally see an outer coefficient which is a 2, and we never see inner coefficients larger than 5.

We intend to present a more satisfactory explanation in terms of renormalisation in a future paper, but this requires studying how all invariant circles break up, not just the boundary ones.

## 5. Behaviour as parameters change

### 5.1. *Variation of $\omega_{\min}$ with $k$*

Fig. 6 shows how $\omega_{\min}[0/1, 1/2]$ varies with $k$ in the standard map. It appears to be a strictly increasing but discontinuous function of $k$. The discontinuities occur every time $\omega_{\min}$ reaches a noble. Since these discontinuities correspond to the destruction of the last rotational invariant circle between two neighbouring island chains, this is consistent with the conjecture that noble circles are the most robust (section 2.4). Note however that our method of locating boundary circles slightly depends on this conjecture, and hence the data in this section does not provide any new evidence in its support.

Note that after $\alpha_1 = (p_0 + \gamma p_1)/(q_0 + \gamma q_1)$ (where $q_1 > q_0$), the next most "important" noble between $p_0/q_0$ and $p_1/q_1$ is $\alpha_2 = (\gamma p_0 + p_1)/(\gamma q_0 + q_1)$ (where $\gamma = (\sqrt{5} + 1)/2$ is the golden mean). They differ by an extra 2 in the continued fraction expansion, e.g. between $\frac{1}{4}$ and $\frac{1}{3}$ we have $[3,1,1,1,\ldots]$ and $[3,2,1,1,\ldots]$. This is the reason why the jumps in fig. 6 appear to take place in two main stages: the first corresponds to the breakup of the $[a_1,\ldots,a_n,1,1,1,\ldots]$ circle and the second to that of $[a_1,\ldots,a_n,2,1,1,\ldots]$. Thus at about $k \simeq 0.904$ the $[3,1,1,1,\ldots]$ circle disappears, to be followed by the $[3,2,1,1,\ldots]$ circle at $k \simeq 0.912$. The reason that the $[a_1,\ldots,a_n,1,1,1,\ldots]$ circle breaks up first is presumably that it is closer to the 0/1 resonance. We

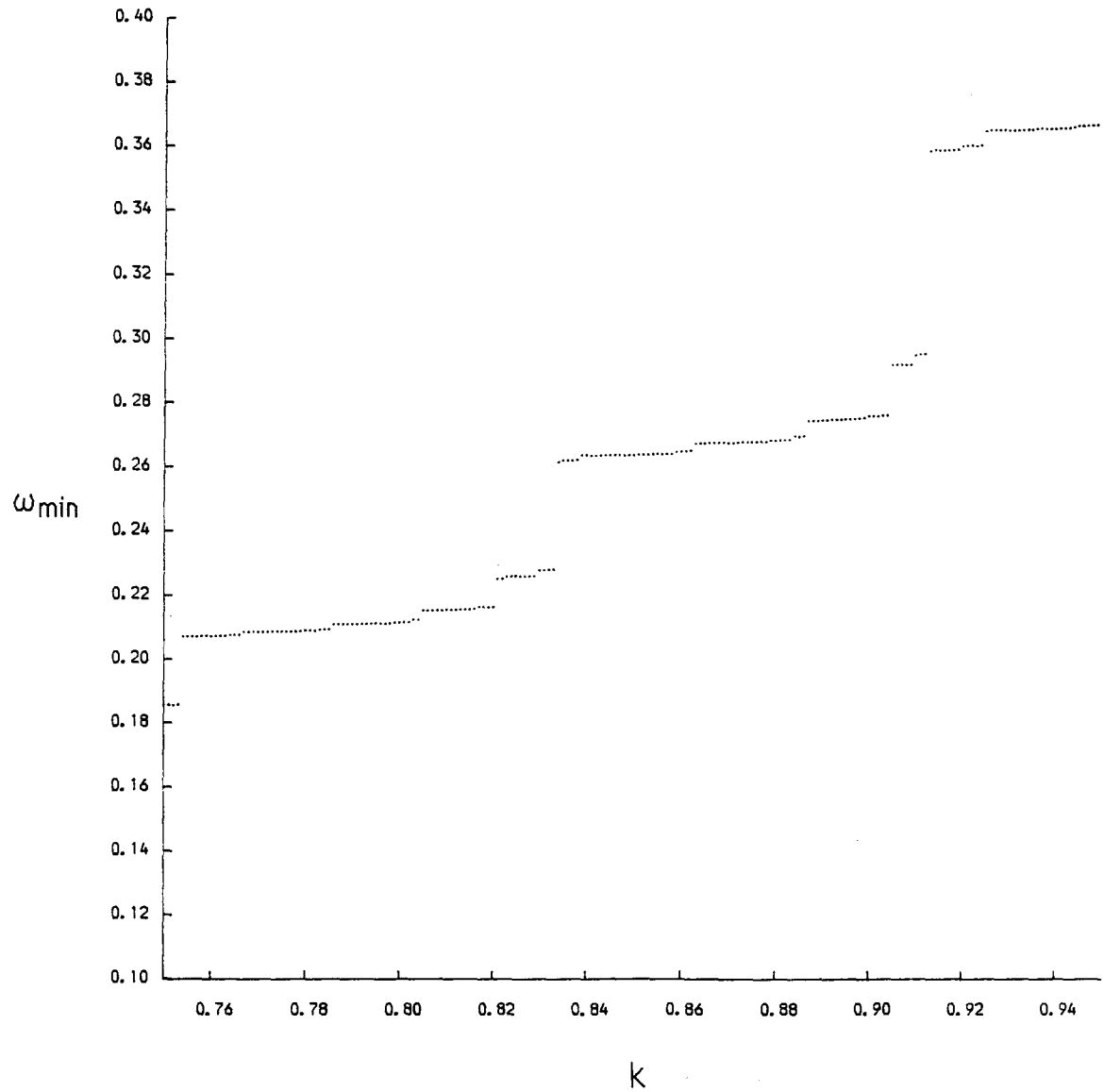


Fig. 6. $\omega_{min}[0/1,1/2]$ against $k$ for the standard map.

believe that it is this phenomenon which gives rise to the occasional 2 in the outer coefficients, rather than having all 1's as our heuristic explanation predicts.

### 5.2. *Parameter scaling*

As mentioned in section 2.3 the breakup of a noble invariant circle appears typically to be governed by a universal one parameter family [4, 5]. Thus we expect to see universal scaling in the neighbourhood of the discontinuities of $\omega_{min}$. Since we need to apply two renormalisations at a time to stay on the same side of the critical noble circle we should see:

$$\omega_c - \omega_{min}(k) = (k_c - k)^{\eta}\varphi(\log_{\delta^2}(k_c - k)), \tag{5.1}$$

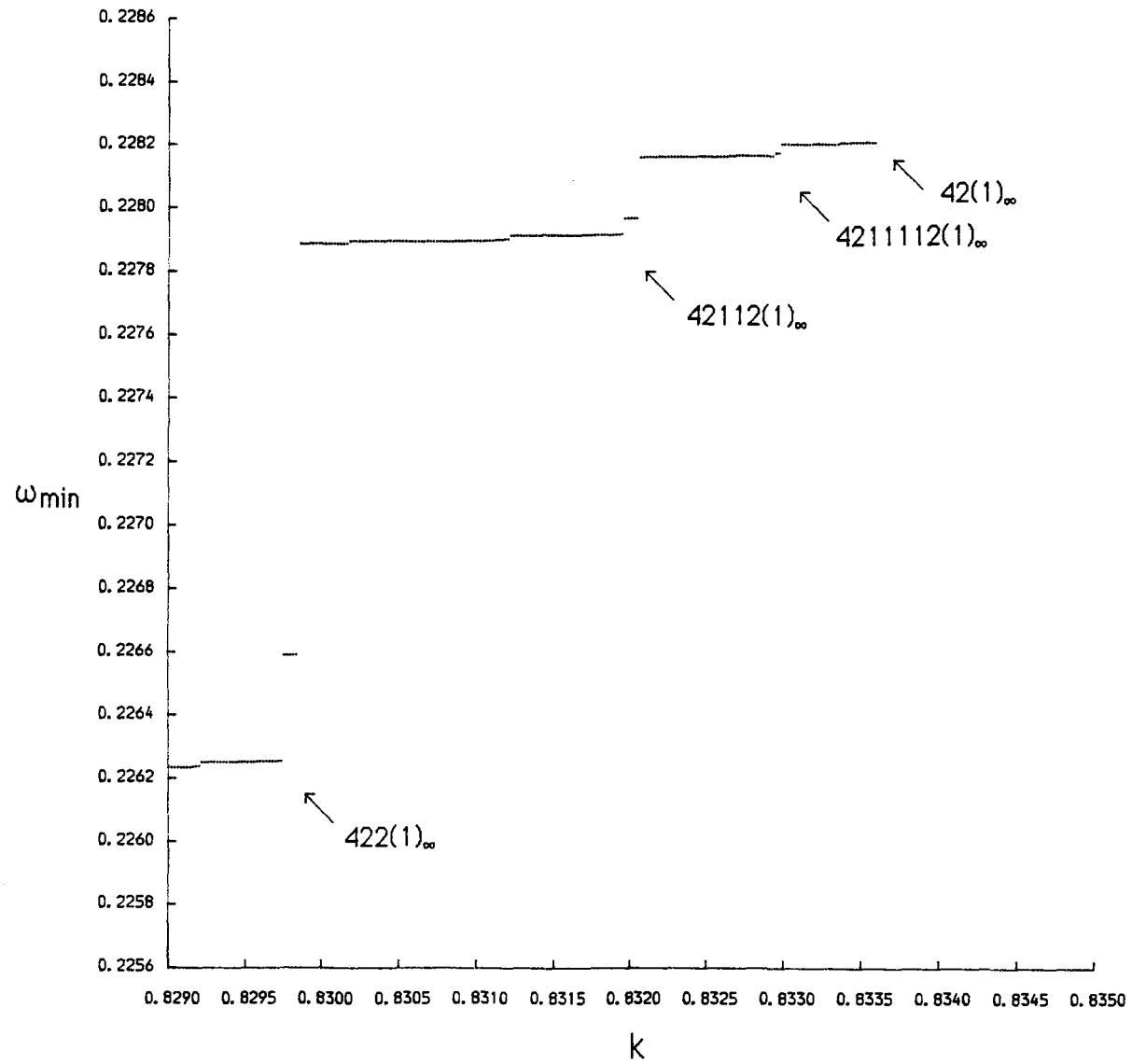


Fig. 7. A detail of fig. 6 leading up to the breakup of the $[4,2,(1)_\infty]$ circle at $k \simeq 0.8336$. The breaking points of three other noble circles are also marked.

where $\omega_c = \omega_{\min}(k_c)$ is the rotation number of a critical noble circle which breaks up at parameter value $k_c$, $\eta = \log_{\delta^2}\gamma^4 \simeq 1.976$, $\delta \simeq 1.62795$ is the unstable eigenvalue of the golden fixed point of the renormalization, and $\varphi$ is a universal function of period 1, i.e. $\varphi(x+1) = \varphi(x)$.

Figure 7 shows the detail of fig. 6 just before the breakup of the $\omega_c = [4,2,1,1,1,\ldots]$ circle at $k_c \simeq 0.8336023\ldots$. We see that leading up to $k_c$ there is an accumulation of other discontinuities of $\omega_{\min}$. Amongst these there is a family of jumps corresponding to rotation number $\omega_n = [4,2,(1)_{2n}, 2,1,1,1,\ldots]$, where by $(1)_{2n}$ we mean $2n$ coefficients which are a 1. Note that $\omega_n$ is obtained from $\omega_{n+1}$ by two renormalisations of its tail. Thus the parameter values $k_n$ at which the discontinuities to $\omega_n$ occur should accumulate geometrically to $k_c$ with ratio $\delta^2 \simeq 2.6504$. Since

$(\omega_c - \omega_n) \sim \gamma^{4n}$, this gives $\omega_c - \omega_n = (k_c - k_n)^\eta$ as in (5.1). In fact we observe that $k_n$ accumulates to $k_c$ with ratio about $2.6 \pm 0.1$, thus giving $\omega_c - \omega_n = (k_c - k_n)^\mu$ with $\mu \simeq 2.0 \pm 0.1$ which agrees well enough with the renormalisation predictions given the lack of accuracy in these calculations. The almost parabolic nature of this accumulation of discontinuities is readily apparent in fig. 7.

## 6. Scaling near boundary circles

### 6.1. *Scaling for critical noble circles*

Noble critical circles exhibit a rich scaling structure. Here, we shall briefly recall those aspects which are relevant to our work on boundary circles. For more details see [3,4,5,19].

Since it is the most relevant to the decay of correlations, let us first consider Mather's $\Delta W$ [13]. Given a rational $p/q$ we define $\Delta W_{p/q}$ to be the difference in action between the minimax and the minimizing Birkhoff periodic orbits of rotation number $p/q$. Mather [13] shows that for an irrational $\omega$, if $p_n/q_n \to \omega$ as $n \to \infty$ then $\Delta W_{p_n/q_n}$ converges to a limit as $n \to \infty$. This limit is independent of the sequence $p_n/q_n$ and thus we may define $\Delta W_\omega$ to be this limit. $\Delta W_\omega$ is then defined for all rotation numbers $\omega$, and is continuous at $\omega$ irrational. Mather also shows that $\Delta W_\omega = 0$ if and only if there is a rotational invariant circle of rotation number $\omega$. $\Delta W$ also has a dynamical interpretation as a flux of area [9,10]. Thus for $\omega$ irrational $\Delta W_\omega$ is the flux across the cantorus of rotation number $\omega$. For $p/q$ rational $\Delta W_{p/q}$ is the flux across the $p/q$ island chain. In both cases if $\Delta W = 0$ then there is a circle of that rotation number, and hence the flux is zero. This interpretation of $\Delta W$ is useful in the Markov model of transport in the irregular components, and knowledge about the scaling behaviour of $\Delta W$ can be used to make predictions about the decay of correlations (see section 6.3). Consider a critical noble circle of rotation number $\omega$. Let $p_n/q_n$ be the convergents of $\omega$ and for notational simplicity write $\Delta W_n = \Delta W_{p_n/q_n}$. By the above $\Delta W_n \to 0$ as $n \to \infty$. In fact one observes that this convergence is asymptotically geometric with a universal ratio. Thus

$$\Delta W_n \sim (\alpha\beta)^{-n}. \tag{6.1}$$

Here $\alpha \simeq -1.4148360\ldots$ and $\beta \simeq -3.0668882\ldots$. Since for a noble, $q_n \sim \gamma^n$ where $\gamma = (\sqrt{5}+1)/2$ is the golden mean, we also have

$$\Delta W_n \sim (q_n)^{-\xi}, \tag{6.2}$$

with $\xi = \log_\gamma(\alpha\beta) \simeq 3.0499\ldots$.

One also finds coordinate scaling around certain points of critical noble circles. Thus for instance consider the point where the circle crosses the dominant reflection line. If we choose appropriate coordinates (normal reflection coordinates [4,5,19]) then the structure around this point will be asymptotically self similar, scaling with $\beta$ along the dominant reflection line and with $\alpha$ across this line. Furthermore this self similarity is universal, i.e. independent of the choice of map.

For the standard map this scaling can in fact be seen directly, without actually making a coordinate change. Recall that $\{x = 0\}$ is a dominant symmetry line. Let $(0, y_n)$ be the position of the $p_n/q_n$ periodic orbit of non-negative residue. Then $y_n \to y$ as $n \to \infty$ where $(0, y)$ is the point at which the noble circle crosses the dominant line. Let $x_n$ be the $x$ coordinate of the nearest point of this periodic orbit to the dominant reflection line. One then observes

$$\begin{aligned} (y_n - y) &\sim (\beta)^{-n} \sim (-1)^n (q_n)^{-\eta}, \\ x_n &\sim (\alpha)^{-n} \sim (-1)^n (q_n)^{-\zeta}, \end{aligned} \tag{6.3}$$

where $\alpha$ and $\beta$ are as above and $\eta = \log_\gamma(-\beta) \simeq 2.329\ldots$ and $\zeta = \log_\gamma(-\alpha) \simeq 0.721\ldots$.

Finally recall from section 3.3 that if $R_n$ is the residue of the $p_n/q_n$ periodic orbit of non-negative residue, then for a critical noble circle $R_n \to R^* \simeq 0.250089\ldots$. This convergence is also asymptotically geometric with ratio $\delta' \simeq -0.61083\ldots$.

All of the above may readily be explained by a fixed point of the renormalization operator $N_1$ [4, 5, 19].

Similar behaviour, but of course with different scaling constants, is observed for any critical circle whose rotation number has a continued fraction with a constant tail e.g. $[a_1, \ldots, a_n, (2)_\infty]$. Such behaviour is governed by the relevant fixed points of the renormalisation. If the tail has a periodic behaviour, e.g. $[a_1, \ldots, a_n, (1,2)_\infty]$, then the above scaling will show an asymptotically periodic behaviour, determined by the corresponding periodic orbit of the renormalisation semi-group.

### 6.2. *Scaling near boundary circles*

We looked at the behaviour of $\Delta W_n$, $(y_n - y)$, $x_n$ and $R_n$ (all defined as in the previous section)

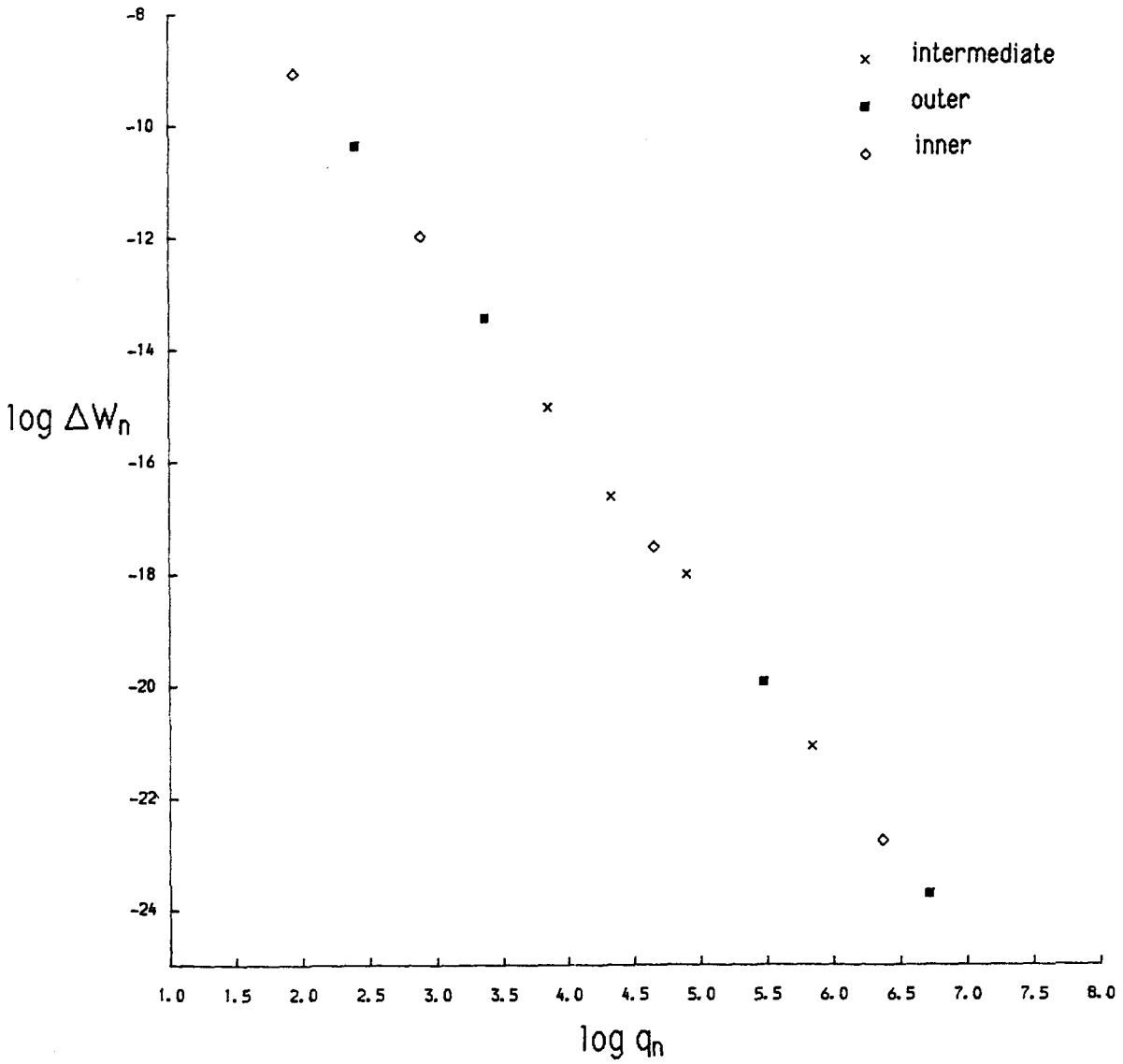


Fig. 8. The behaviour of $\Delta W$ for rationals approximating $\omega_{\min}[0/1, 1/2]$ for the standard map at $k = 0.9$.

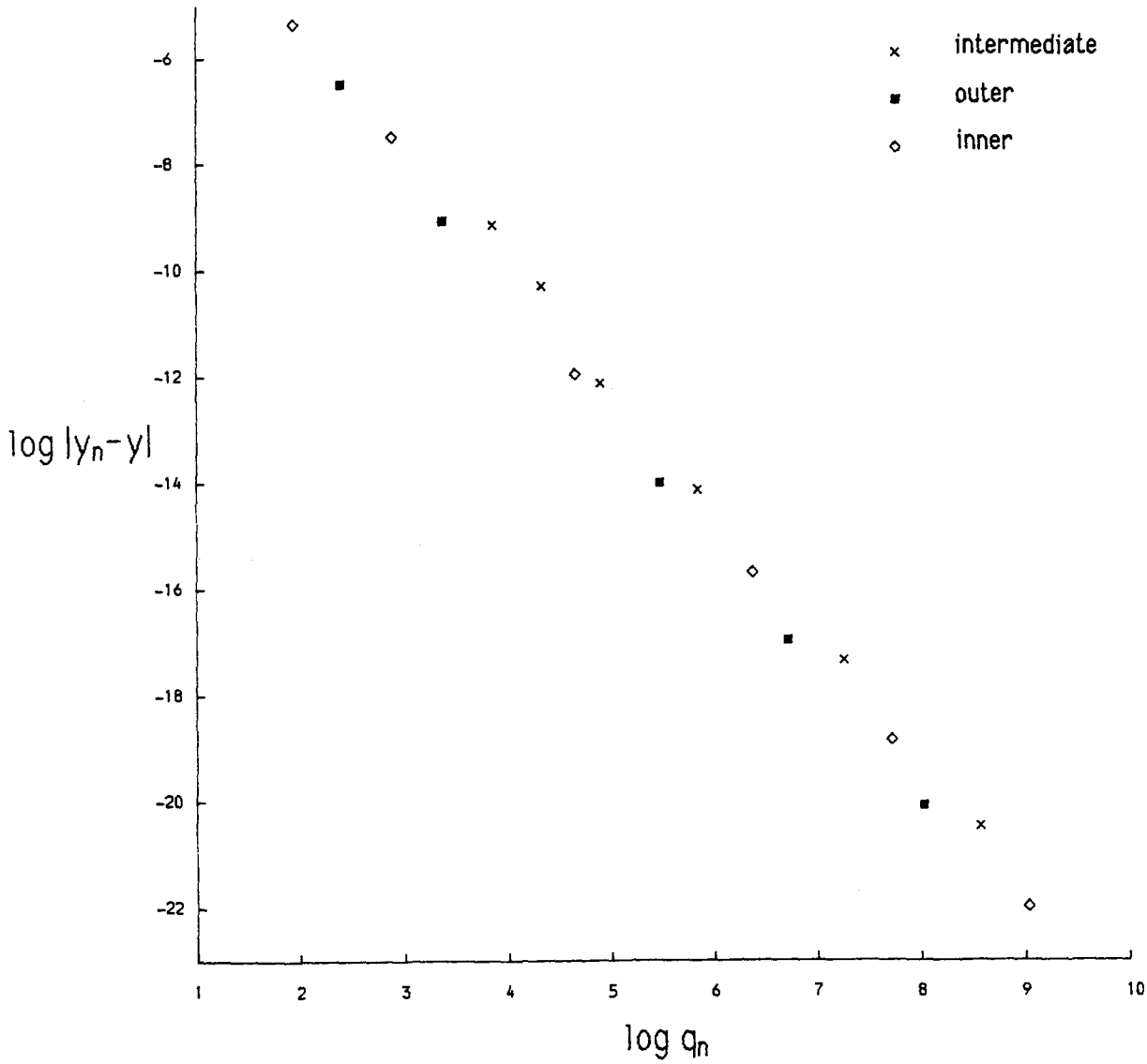


Fig. 9. Scaling along the dominant symmetry line for the $\omega_{\min}[0/1,1/2]$ circle for the standard map at $k = 0.9$.

near boundary circles. The first three quantities all converge to zero as $n \to \infty$, and for boundary circles we find they scale against $q_n$ with small fluctuations. As expected the residues $R_n$ neither converge to a limit, nor go to infinity as $n \to \infty$. They turn out to behave in a complicated fashion which we consider in section 7. Note that in general $q_n$ does not grow in a nice fashion with $n$, and thus no scaling is seen in terms of $n$ for any of the above quantities.

Figs. 8, 9, and 10 show a plot of $\log \Delta W_n$, $\log |y_n - y|$ and $\log |x_n|$ against $\log q_n$ for $p_n/q_n$ periodic orbits converging to $\omega_{\min}[0/1,1/2]$ for the standard map at $k = 0.9$. We have included the intermediate rationals as well as the inner and outer convergents. We see that there is a good fit

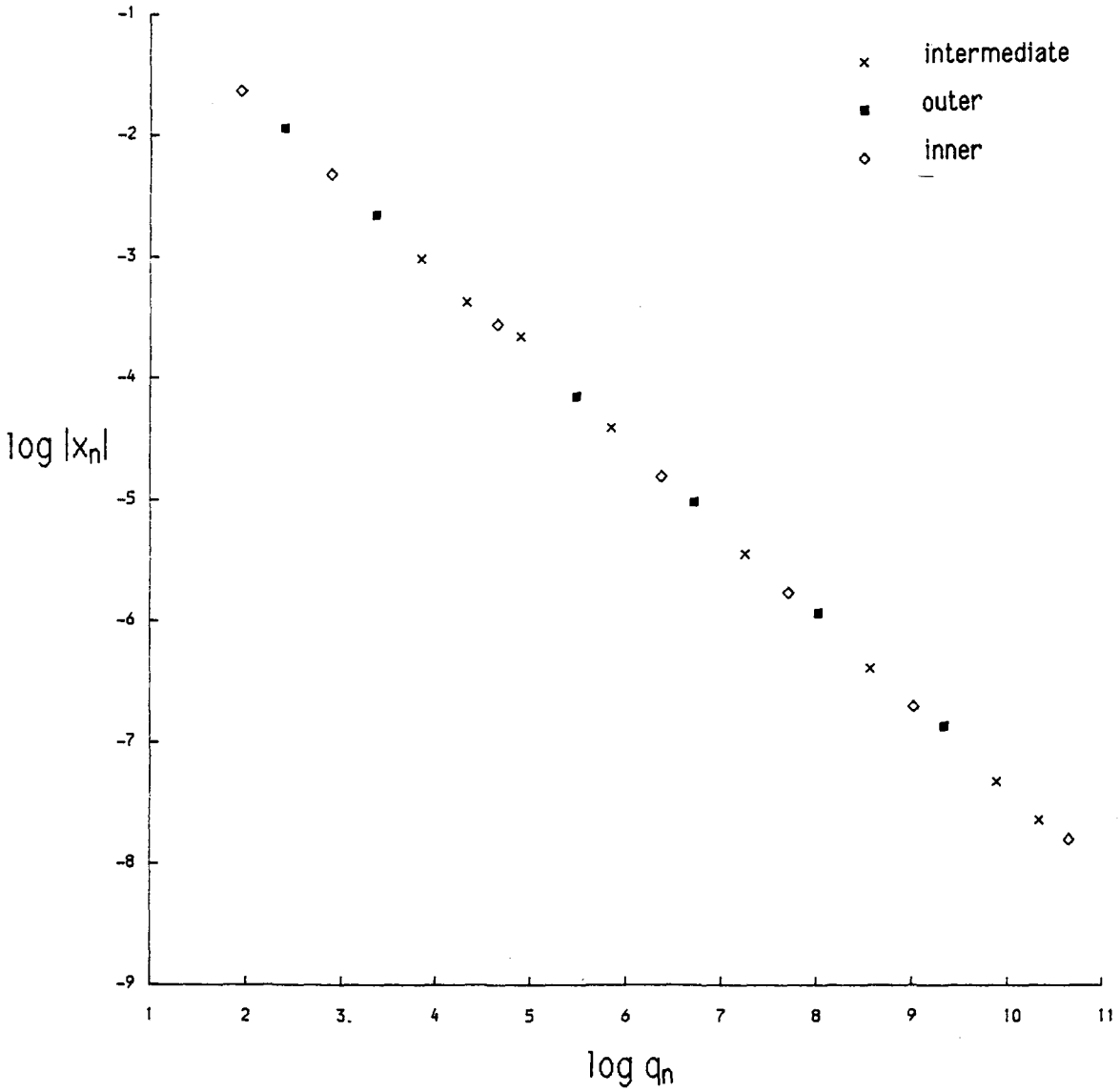


Fig. 10. Scaling across the dominant symmetry line for the $\omega_{\min}[0/1, 1/2]$ circle for the standard map at $k = 0.9$.

to

$$\begin{aligned} &\Delta W_n \sim (q_n)^{-\xi}, \quad \xi \simeq 3.1, \\ &|y_n - y| \sim (q_n)^{-\eta}, \quad \eta \simeq 2.3, \\ &|x_n| \sim (q_n)^{-\zeta}, \quad \zeta \simeq 0.72. \end{aligned} \tag{6.5}$$

If we restrict ourselves to either only the outer convergents or the inner convergents then the fit is even better, particularly for $|y_n - y|$. Similar behaviour was observed for all the other boundary circles that we looked at. To get a better feel for the variations from (6.5) we considered the follow-

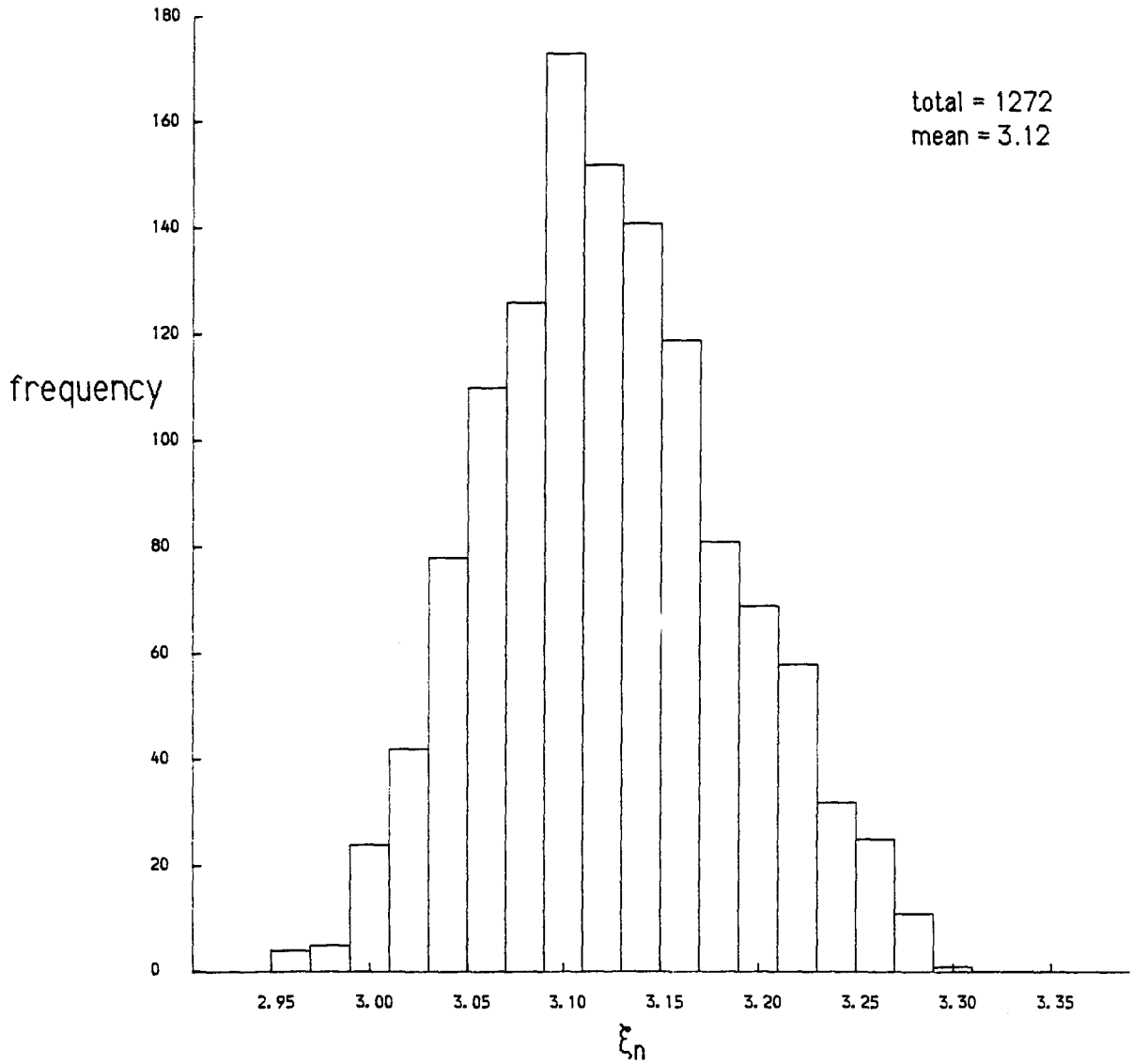


Fig. 11. Distribution of $\xi_n$ for the outer convergents of boundary circles in the standard map.

ing quantities:

$$\xi_n = \frac{\log(\Delta W_{n+2}/\Delta W_n)}{\log(q_{n+2}/q_n)},$$

$$\eta_n = \frac{\log(|y_{n+2} - y|/|y_n - y|)}{\log(q_{n+2}/q_n)},$$

$$\zeta_n = \frac{\log(|x_{n+2}|/|x_n|)}{\log(q_{n+2}/q_n)},$$

where $p_n/q_n$ is an outer convergent and $p_{n+2}/q_{n+2}$ is the next outer convergent. Figs. 11, 12 and 13 give the distributions of $\xi_n$, $\eta_n$ and $\zeta_n$ that we found. The ones for inner convergents can also be calculated and look much the same. Note that these figures are meant only as rough indications of the behaviour seen; the data is too crude to make any claims of universality.

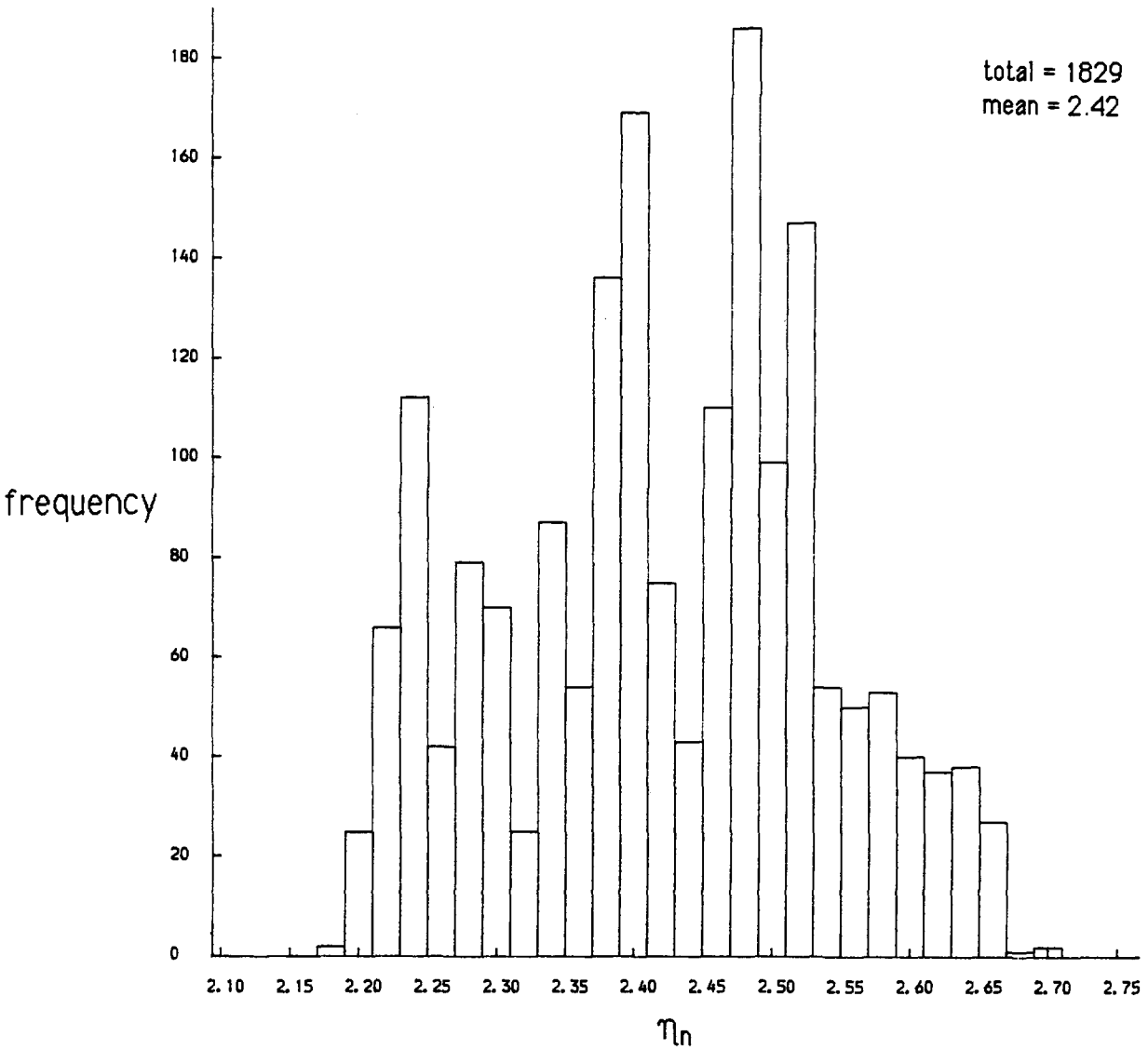


Fig. 12. Distribution of $\eta_n$ for the outer convergents of boundary circles in the standard map.

Recall that for nobles $\xi_n \to \log_\gamma(\alpha\beta)$ as $n \to \infty$ and similarly for $\eta_n$ and $\zeta_n$. There is however no evidence of any such convergence to a limit for boundary circles.

Note that although figs. 11, 12 and 13 show quite a wide spread in $\xi_n$, $\eta_n$ and $\zeta_n$, this could be somewhat misleading. Figs. 8, 9, and 10 seem to suggest that the variations in these slopes cancel out to some extent and thus over several levels the scaling is much better than might be indicated by figs. 11 to 13. This overall scaling given by (6.5) is remarkably close to that of critical noble circles. It is interesting that Shenker and Kadanoff [3] calculate this scaling for a $[a_1, \ldots, a_n, (2)_\infty]$ circle and obtain $\eta = 2.34 \pm 0.01$ and $\zeta = 0.72 \pm 0.1$; $\xi$ should then be given by $\eta + \zeta = 3.06 \pm 0.11$. Thus from their data the scaling for $(1)_\infty$ and $(2)_\infty$ circles is indistinguishable. In fact if the calcula-

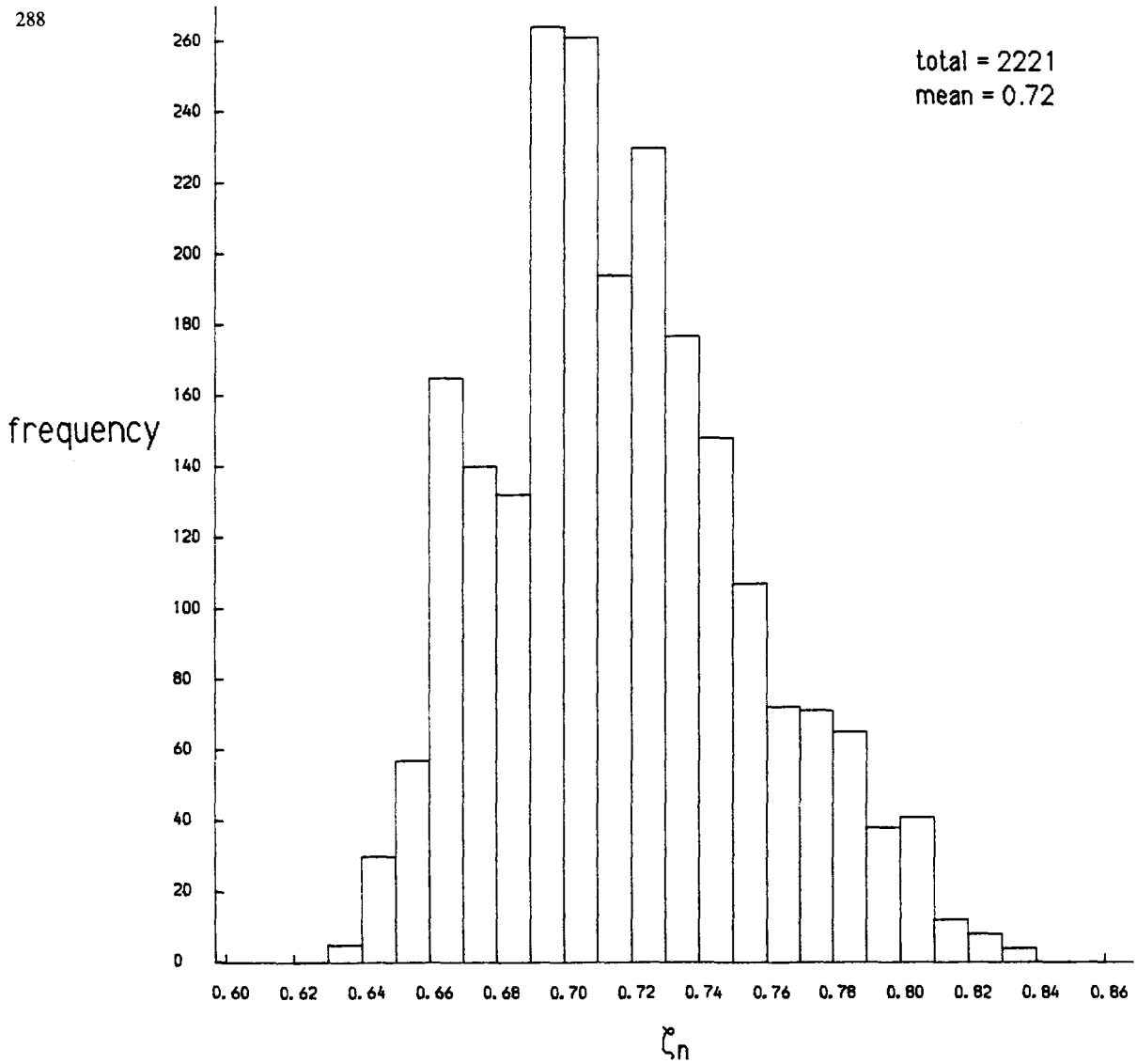


Fig. 13. Distribution of $\zeta_n$ for the outer convergents of boundary circles in the standard map.

Table IV
Scaling exponents for a number of critical circles with continued fractions with periodic tails

| Tail | $\xi$ | $\eta$ | $\zeta$ |
|---|---|---|---|
| $(1)_\infty$ | 3.050 | 2.329 | 0.7211 |
| $(2)_\infty$ | 3.063 | 2.345 | 0.7173 |
| $(3)_\infty$ | 3.09 | 2.38 | 0.709 |
| $(1,2)_\infty$ | 3.10 | 2.39 | 0.709 |
| $(1,3)_\infty$ | 3.19 | 2.49 | 0.694 |
| $(1,4)_\infty$ | 3.26 | 2.59 | 0.680 |
| $(1,5)_\infty$ | 3.35 | 2.69 | 0.667 |
| $(2,3)_\infty$ | 3.09 | 2.39 | 0.710 |

tion is done with higher precision the scaling constants for the two types of circles are seen to be different, but very close. We thus also calculated the scaling for the $(3)_\infty$, $(1,2)_\infty$, $(1,3)_\infty$, $(1,4)_\infty$, $(1,5)_\infty$ and $(2,3)_\infty$ circles, all of which give scaling constants within a few percent of the corresponding ones for nobles (table IV). The scaling of $\Delta W_n$, $(y_n - y)$ and $x_n$ thus appears to be remarkably similar for all critical circles, or at least for those with fairly small coefficients in the continued fraction expansion. The simplest explanation for this is that all the relevant fixed and periodic points of the renormalisation semi-group which govern the breakup of these circles are in some sense close to each other in the space of area-preserving maps.

### 6.3. *Decay of correlations*

Since $\Delta W_\omega$ is a flux of area, it can be used to predict transition times across the barrier (cantorus or island chain) of rotation number $\omega$. One can thus subdivide an irregular component into a discrete number of regions and, assuming that mixing in each region is fast compared to the movement across barriers, obtain a Markov chain model of transport in irregular components [9, 10, 27]. Using this model and the scaling of $\Delta W$ near critical noble circles, Hanson, Cary and Meiss [28] make predictions for the distribution of first passage times and the decay of correlations in an irregular component bounded by critical noble circles. Unfortunately their analysis cannot be directly applied to general boundary circles since they require $\Delta W$ to scale with $n$, whilst for boundary circles we only get scaling with respect to $q_n$. However it is also possible to set up a continuous version of this model, leading to an inhomogeneous diffusion equation [6]. In the noble case the predictions of the two models agree and we expect the continuous model to be equally valid for the case of boundary circles, subject to the scaling hypothesis $\Delta W \sim q^{-\xi}$ (6.5). See appendix A for an analysis of this continuous model. It predicts that:

i) typical initial distributions decay pointwise like $t^{-\xi}$.

ii) the autocorrelation of typical continuous functions decays like $t^{-(\xi-1)}$.

Sadly these predictions disagree quite badly with the results of numerical experiments [7, 8]. They find that the distribution of first return times decays roughly like $t^{-2.5}$, phase space distributions decay like $t^{-1.5}$ and autocorrelations like $t^{-0.5}$. We would conjecture that this disagreement is due to the fact that a linear Markov chain model only considers orbits trapped near to one boundary circle and ignores the possibility of their getting stuck near periodic boundary circles around nearby island chains. A better model would thus be to try a branching binary tree. Meiss and Ott [12] have analysed the case of a self-similar binary tree (see also [27]). Using branching ratios measured for the $(1,7):(1,7)\ldots$ bifurcation sequence and our scaling for each boundary circle, this model predicts decay laws much closer to those observed in numerical experiments.

## 7. Behaviour of residues

For boundary circles there is no convergence of the residues of approximating periodic orbits to any limiting value or periodic behaviour. This is to be expected, as not all boundary circles are governed by fixed or periodic points of the renormalisation.

The residues do however turn out to be reasonably well behaved. Let $f$ be an area-preserving twist map with a boundary circle of rotation number $\omega = [a_1, a_2, \ldots]$. As in section 6 let $R_n$ be the residue of the $p_n/q_n = [a_1, a_2, \ldots, a_n]$ periodic orbit of non-negative residue, $\omega_n = [a_{n+1}, a_{n+2}, \ldots]$ and $\nu_n = [a_n, a_{n-1}, \ldots, a_1]$. Fig. 14 shows a plot of $R_n$ against $\omega_n$ and $\nu_n$ for $a_n$ an outer coefficient. The picture for inner coefficients is very similar. It appears that $R_n$ is a function of $\omega_n$ and $\nu_n$. Similarly $R_{n-1}$ appears to be a func-

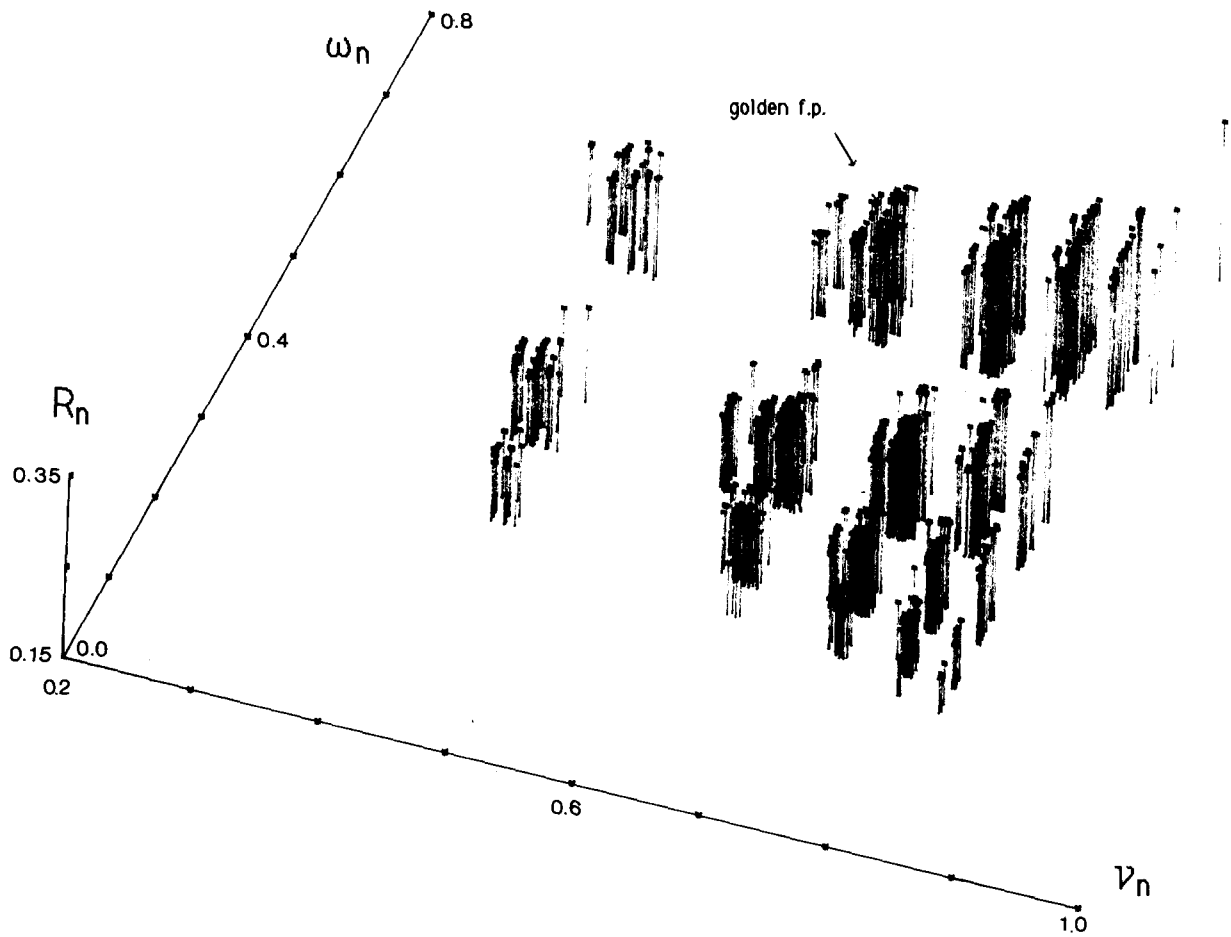


Fig. 14. $R_n$ against $\nu_n$ and $\omega_n$ for outer convergents to boundary circles in the standard map. Each plotted point is joined by a straight line to the plane $R_n = 0.15$. The axes are marked in units of 0.1.

tion of $\omega_n$ and $\nu_n$ (fig. 15). Indeed for sufficiently large $n$ we expect every observable of the pair $(T^{q_{n-1}}R^{q_{n-1}}, T^{q_n}R^{q_n})$ (where $R(x, y) = (x - 1, y)$) to depend only on $\omega_n$ and $\nu_n$.

Another way to say this is that we believe that in the space of pairs $(U, T)$ of area-preserving maps there is a special set $\{(U,T)_{\omega,\nu}: \omega, \nu \in (0,1)\}$ which can be parameterised by two numbers $\nu$ and $\omega$ in $(0,1)$, such that if $F$ has a boundary circle of rotation number $\omega_0$ then $N_{a_n} \ldots N_{a_1}(F, R) \to (U, T)_{\omega_n, \nu_n}$.

Similar ideas have been suggested for the structure of the boundary of Siegel disks [26], and we believe that numerical results for critical circle maps [29, 30] and for the quasiperiodic Schrödinger equation [31] can also be interpreted this way. See also (ref. [32]).

In view of this we can plot projections of this subset, for example into the $(R_n, R_{n-1})$ plane. A coherent structure is apparent, but different parts of this structure seem to overlap (and we therefore do not show this picture). To separate these out we can use either $\nu_n$ or $\omega_n$ (or in fact since $\nu_n$ and $\omega_n$ are largely determined by $a_n$ and $a_{n+1}$ respectively, the latter will do). Fig. 16 shows an example of the sort of picture one obtains. One can see

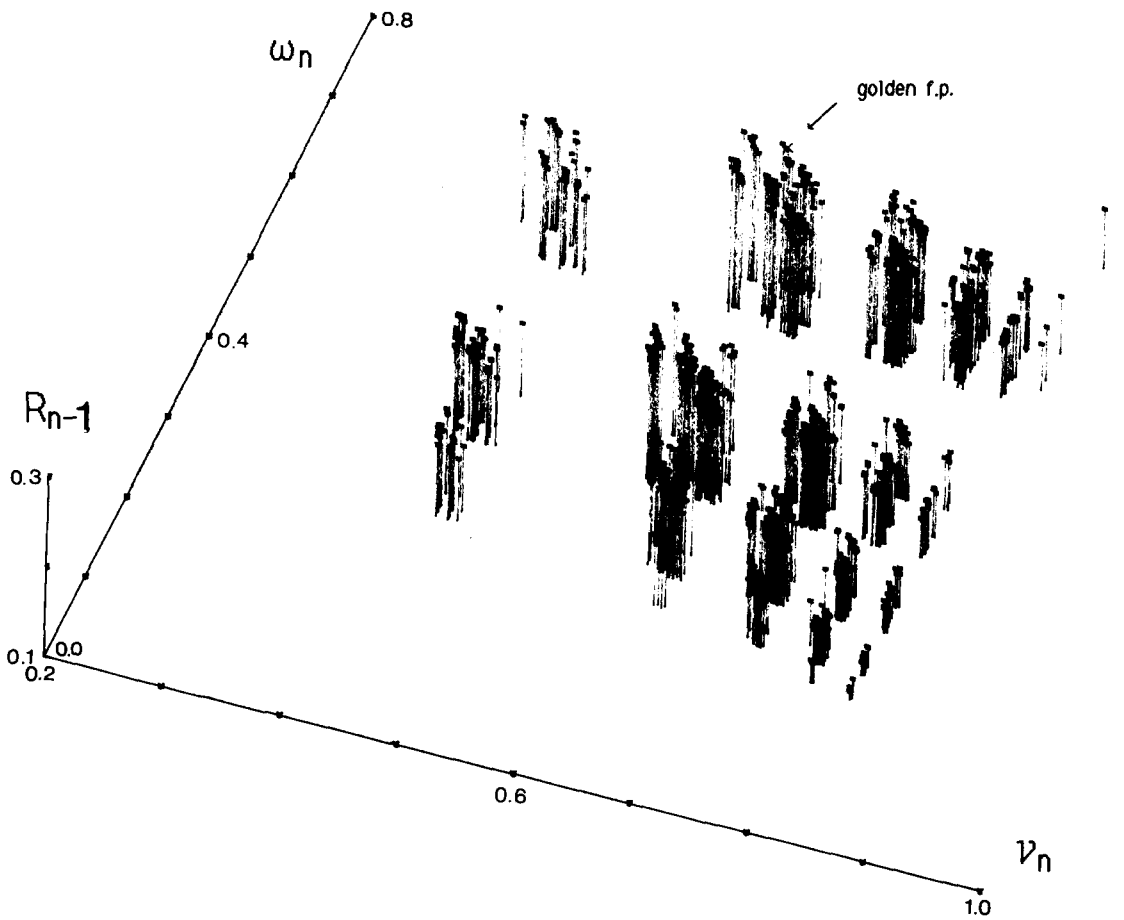


Fig. 15. $R_{n-1}$ against $\nu_n$ and $\omega_n$ for outer convergents to boundary circles in the standard map. Each plotted point is joined by a straight line to the plane $R_n = 0.1$. The axes are marked in units of 0.1.

that this set is sharply bounded by several surfaces. One of these is presumably the stable manifold of the critical noble fixed point. We have so far not determined what the others are, but we conjecture that they are all pre-images of the stable manifold of the noble fixed point under a finite sequence of renormalisation maps. The advantage of using $R_n$, $R_{n-1}$, $\nu_n$ and $\omega_n$ is that we can set up an exactly solvable approximate renormalisation scheme in this four-dimensional space which seems to give very accurate results [33, 25]. Thus we should be able to determine where the stable and unstable manifolds of the various fixed and periodic orbits of the renormalisation lie. This should allow us to identify the boundaries of the set in fig. 16 and in turn lead to an explanation of the restrictions on the continued fraction of boundary circles given in section 4.2. Indeed it seems that the residues are continuous in both $\omega$ and $\nu$ (though only defined on a Cantor set). It is interesting that in the analogous renormalisation for the boundary of Siegel disks, for arbitrary rotation number, one observes behaviour continuous in $\omega_n$ but not in $\nu_n$ (in this case almost all $\omega$ and $\nu$ occur) [26]. It would be interesting to see whether if fig. 14 were extended to all rotation numbers (i.e. to all

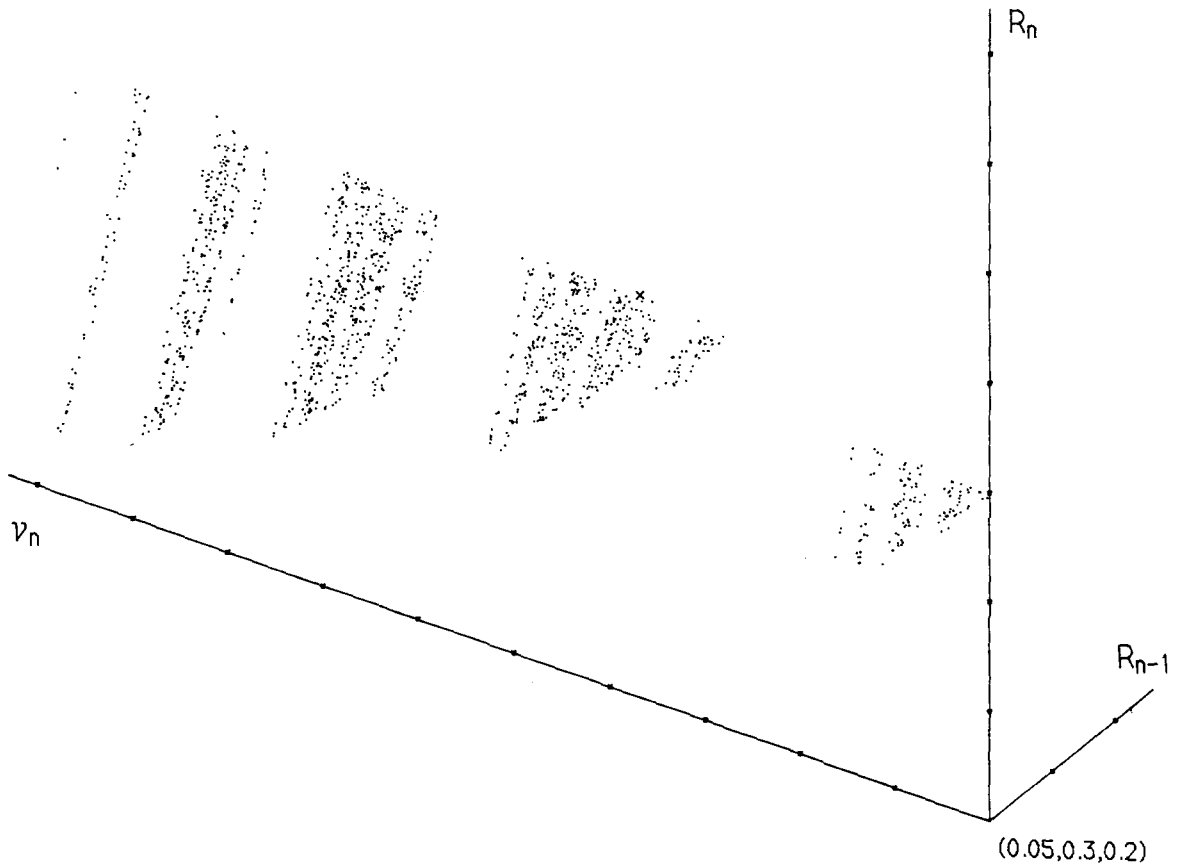


Fig. 16. A plot of $R_n$, $R_{n-1}$ and $\nu_n$ for outer convergents to boundary circles in the standard map. The golden fixed point is marked by a cross. The axes are marked in units of 0.05.

$(\omega_n, \nu_n) \in [0,1] \times [0,1]$) this phenomenon would also be seen in this problem.

## 8. Conclusion

We have shown numerical evidence that boundary circles for area-preserving maps have rotation numbers of a special form. The "outer" coefficients of the continued fraction expansion appear to be always 1 or 2, the "inner" coefficients a 1, 2, 3, 4 or 5. This has recently been confirmed by Grassberger (private communication), using a different method for locating boundary circles, based on Converse KAM [34]. We have also presented evidence for scaling properties near boundary circles. In particular the difference of actions for convergent periodic orbits appears to scale like:

$$\Delta W_{p_n/q_n} \sim C(q_n)^{-\xi}, \quad \xi \simeq 3.1.$$

This is a vital ingredient for calculations of the long-time relaxation to equilibrium in Markov models of irregular components.

Finally we have indicated that under the sequence of renormalisation transformations corresponding to a boundary circle, maps appear to converge to a universal set of maps which can be parameterised by the renormalised rotation number $\omega$, and a "memory" of the past renormalisation $\nu$. We believe that this is but part of a larger set corresponding to all critical circles and intend to investigate further.

**Acknowledgements**

The authors are grateful to J.D. Meiss and J.R. Cary for a number of helpful conversations. This work was supported in part by US DOE Grant No. DE-FG03-85ER13402. We thank the U.K. Science and Engineering Research Council (SERC) for provision of computing facilities. J. Stark also gratefully acknowledges the financial support of SERC.

## Appendix A

*Chirikov's model*

Chirikov's model is an inhomogeneous diffusion equation for a phase space density $f$:

$$\frac{\partial f}{\partial t} = \frac{\partial}{\partial A} A^{\kappa} \frac{\partial f}{\partial A}, \quad \kappa = \frac{2\xi - 1}{\xi - 1}. \tag{6.6}$$

Here $A$ is a coordinate measuring the accessible area of the irregular component up to the boundary circle. The motivation for this is that if $\Delta W_n \sim (q_n)^{-\xi}$ and one takes a coordinate $r$ to interpolate $(\log q_n)$ (note that the boundary circle is then at $r = +\infty$) then:

$$\Delta W(r) \sim \mathrm{e}^{-\xi r},$$
$$A(r) \sim \Delta W \cdot q_n \sim \mathrm{e}^{-(\xi-1)r}.$$

The "major" turnstiles are roughly speaking evenly distributed in $r$, since the $a_n$ appear to be bounded for boundary circles. Thus it is reasonable to model the irregular component by a diffusion problem with effective resistance per unit length in $r$ proportional to $\mathrm{e}^{\xi r}$, and capacitance per unit length in $r$ proportional to $\mathrm{e}^{-(\xi-1)r}$. The equation for the density $f$ is then

$$\frac{\partial}{\partial t}\left(\mathrm{e}^{-(\xi-1)r} f\right) = \frac{\partial}{\partial r} \mathrm{e}^{-\xi r} \frac{\partial f}{\partial r}. \tag{6.7}$$

Transforming coordinates from $r$ to $A$ leads to Chirikov's [8] equation (6.6). Actually Chirikov gave no justification for it and assumed a value of $\kappa$ slightly different from the one derived here. This derivation of the value of $\kappa$ was made independently by Meiss [private communication]. Note that $\kappa > 2$ since $\xi > 1$.

Meiss also derived a Green's function $G(A, t, A_0)$ for this diffusion equation, i.e. a solution with initial condition $G(A, 0, A_0) = \delta(A - A_0)$. It is

$$G(A, t, A_0) = (\kappa - 2) \frac{\zeta\zeta_0}{\sqrt{(AA_0)}} \mathrm{e}^{-(\zeta_0)^2 - \zeta^2} I_p(2\zeta_0\zeta), \tag{6.8}$$

where $\zeta = A^{-(\kappa-2)/2}/(\kappa - 2)\sqrt{t}$ and $\zeta_0$ similarly defined, $p = (\kappa - 1)/(\kappa - 2)$ and $I_p$ is the modified Bessel function. Note that using our value for $\kappa$ we get $p = \xi$, and also that since $\kappa > 2$, the boundary circle is at $\zeta = +\infty$.

For fixed $A$ and $A_0$, $G(A, t, A_0)$ decays as $t^{-(p+1)}$ for $t \gg A^{-(\kappa-2)}$, $t \gg A_0^{-(\kappa-2)}$. This is because $I_p(x) \sim (x/2)^p/\Gamma(p+1)$ for small $x$. However this relaxation is non-uniform in $A, A_0$. One has to wait longer before this asymptotic form is attained the smaller $A$ and $A_0$ are. Thus one might find a different behaviour for initial distributions $f_0$ for which $f_0(A) \to f_{00} \neq 0$ as $A \to 0$. The solution for a general initial distribution $f_0(A)$ with $\int f_0(A)\,\mathrm{d}A < \infty$ is:

$$f(A, t) = \int \mathrm{d}A_0 G(A, t, A_0) f_0(A_0).$$

Fix $A$. Because of the $\mathrm{e}^{-(\zeta_0)^2}$ factor in $G$, the main contribution is from $\zeta_0 \leq 1$ ($I_p(x)$ grows only like $\mathrm{e}^x/\sqrt{(2\pi x)}$ as $x \to \infty$). Now for $t \gg A^{-(\kappa-2)}$ and $\zeta_0 \leq 1$ we get $2\zeta\zeta_0 \ll 1$. So approximate $I_p(x)$ by its small $x$ form above and change the variable of integration from $A_0$ to $\xi_0$. One obtains

$$f(A, t) \sim \frac{(\kappa - 2)^{1-2p} t^{-p}}{\Gamma(p+1)} \times A^{\kappa-1} \mathrm{e}^{-\zeta^2} \int_0^{\infty} \zeta_0 \mathrm{e}^{-(\zeta_0)^2} f_0(A_0)\,\mathrm{d}\zeta_0.$$

The integrand is dominated by $\zeta_0 \leq 1$ and $\int_0^{\infty} \zeta_0 \mathrm{e}^{-(\zeta_0)^2}\,\mathrm{d}\zeta_0 = \frac{1}{2}$. If $\zeta_0 \leq 1$ then $A_0 \to 0$ as $t \to \infty$. So if $f_0(A) \to f_{00} \neq 0$ as $A \to 0$ then (for fixed $A$):

$$f(A, t) \sim \frac{(\kappa - 2)^{1-2p}}{2\Gamma(p+1)} A^{\kappa-1} f_{00} t^{-p}, \quad \text{as } t \to \infty.$$

Thus general initial distributions decay like $t^{-p}$ pointwise.

So far we have taken the total accessible area to be infinite. If it is finite we still expect relaxation to the equilibrium density $\langle f_0 \rangle$ with the same power law decay for initial distributions $f_0$, with the condition $f_0 \to f_{00} \neq 0$ as $A \to 0$ replaced by $f_0 \to f_{00} \neq \langle f_0 \rangle$, where $\langle f_0 \rangle$ is the average of $f_0$ over the total accessible area of the irregular component.

This model also suggests that for "most" functions $\varphi$ on the phase space the autocorrelation function $C_\varphi(n)$ decays as $n^{-(p-1)}$ as $n \to \infty$:

$$C_\varphi(n) = \int_I (\varphi(x_0) - \langle\varphi\rangle)(\varphi(T^n(x_0)) - \langle\varphi\rangle) \times d\lambda(x_0) \sim n^{-(p-1)} \quad \text{as } n \to \infty, \quad (6.10)$$

where $I$ is an irregular component, $\lambda$ is the measure preserved by $T$ and $\langle\varphi\rangle$ is the average of $\varphi$ over $I$ with respect to $\lambda$. To derive (6.10) write

$$\varphi(T^n x_0) = \int_I \varphi(x)\, \delta(x - T^n(x_0))\, d\lambda(x).$$

Introduce a coordinate $\theta$ such that $dA\, d\theta = d\lambda$. We get

$$C_\varphi(n) = \int_I dA_0 d\theta_0 \int_I dA\, d\theta\, \varphi(x_0) \times \varphi(x)\, \delta(x - T^n(x_0)).$$

Since the Green's function describes how an initial delta function in $A$ spreads, if we assume "phase mixing" in the $\theta$ coordinate it is reasonable to approximate $C_\varphi(n)$ by

$$C_{\varphi^*}(n) = \int_I \int_I dA_0 dA\, \varphi^*(A_0)\varphi^*(A) G(A, n, A_0),$$

where $\varphi^*(A) = \int d\theta\, \varphi(A, \theta)$. Let us evaluate this for the diffusion model. Putting $\zeta = A^{-(\kappa-2)/2}/(\kappa - 2)\sqrt{t}$ and $D = 4(\kappa - 2)^{1-2p}$ we get

$$C_{\varphi^*}(t) = Dt^{-(p-1)} \int_0^\infty \int_0^\infty \varphi^*(A_0)\varphi^*(A)(\zeta\zeta_0)^{1-p} \times e^{-(\zeta_0)^2 - \zeta^2} I_p(2\zeta\zeta_0)\, d\zeta\, d\zeta_0.$$

Since $p > 1$, $\int_0^\infty \int_0^\infty (\zeta\zeta_0)^{1-p} e^{-(\zeta_0)^2 - \zeta^2} I_p(2\zeta\zeta_0)\, d\zeta\, d\zeta_0$ converges, to $C_p$ say. The integrand of $C_{\varphi^*}(t)$ is then dominated by a neighbourhood of $\zeta = 1$, $\zeta_0 = 1$. As $t \to \infty$ with $\zeta, \zeta_0 \sim 1$, then $A, A_0 \to 0$. So if $\varphi^*(A) \to \varphi_0^*$ as $A \to 0$ then

$$C_{\varphi^*}(t) \sim 4(\kappa - 2)^{1-2p} C_p (\varphi_0^*)^2 t^{-(p-1)}, \quad \text{as } t \to \infty.$$

The autocorrelation thus decays with exponent $p - 1$.

In section 6.2 we observed that $p$ is very similar for critical noble circles and for general boundary circles. The predictions of this diffusion model are thus essentially the same as those of Hanson, Cary and Meiss [28] for the neighbourhood of a critical noble circle.

## References


[1] J.M. Greene, A method for determining a stochastic transition, J. Math. Phys. 20 (1979) 1183–1201.

[2] B.V. Chirikov, A universal instability of many dimensional oscillator systems, Physics Reports 52 (1979) 263–379.

[3] S.J. Shenker and L.P. Kadanoff, Critical behaviour of a KAM surface: I Empirical results, J. Stat. Phys. 27 (1982) 631–656.

[4] R.S. MacKay, Renormalisation in Area-Preserving Maps, PhD Thesis, Princeton (1982).

[5] R.S. MacKay, A renormalisation approach to invariant circles in area-preserving maps, Physica 7D (1983) 283–300.

[6] B.V. Chirikov, Chaotic Dynamics in Hamiltonian Systems with Divided Phase Space, Lecture Notes in Physics 179 (Springer, Berlin, 1983) pp. 29–46.

[7] B.V. Chirikov and D.L. Shepelyanski, Correlation properties of dynamical chaos in Hamiltonian systems, Physica 13D (1984) 395–400.

[8] C.F.F. Karney, Long-time correlations in the stochastic regime, Physica 8D (1983) 360–380.

[9] R.S. MacKay, J.D. Meiss and I.C. Percival, Transport in Hamiltonian systems, Physica 13D (1984) 55–81.

[10] D. Bensimon and L.P. Kadanoff, Extended chaos and disappearance of KAM trajectories, Physica 13D (1984) 82–89.

[11] J.D. Meiss, J.R. Cary, C. Grebogi, J.D. Crawford, A.N. Kaufman and H.D.I. Abarbanel, Long time correlations of periodic area-preserving maps, Physica 6D (1983) 375–384.

[12] J.D. Meiss and E. Ott, Markov tree model of transport in area-preserving maps, Physica 20D (1986) 387–402.

[13] J.N. Mather, A criterion for the non-existence of invariant circles, preprint, Princeton, 1982.
[14] Z. Nitecki, Differentiable Dynamics (MIT Press, Cambridge MA, 1971).
[15] V.I. Arnold, Geometric Methods in the Theory of Ordinary Differential Equations (Springer, Berlin, 1983).
[16] M.R. Herman, Sur les Courbes Invariantes par les Difféomorphismes de l'Anneau, vol. 1, Astérisque 103–104 (1983).
[17] R.C. Robinson, Generic properties of conservative systems, Am. J. Math. 92 (1970) 562–603 and 897–906.
[18] G.H. Hardy and E.M. Wright, Introduction to the Theory of Numbers, 5th ed. (Clarendon, Oxford, 1979).
[19] R.S. MacKay, Transition to Chaos for Area-Preserving Maps, in Lecture Notes in Physics 247, J.M. Javett, M. Month and S. Turner, eds. (Springer, Berlin, 1986) pp. 390–454.
[20] J.K. Moser, Stable and Random Motions in Dynamical Systems (Princeton Univ. Press, Princeton, 1973).
[21] G.D. Birkhoff, Proof of Poincaré's geometric theorem, Trans. AMS 14 (1913) 14–22.
[22] J.N. Mather, Existence of quasi-periodic orbits for twist homeomorphisms of the annulus, Topology 21 (1982) 457–467.
[23] S. Aubry and P.Y. Le Daeron, 1983, The discrete Frenkel–Kontorova model and its extensions I: Exact results for the ground states, Physica 8D (1983) 381–422.
[24] R.S. MacKay and J.D. Meiss, Linear stability of periodic orbits in Lagrangian systems, Phys. Lett. A 98 (1984) 92–94.
[25] R.S. MacKay, Exact Results for an Approximate Renormalisation scheme, in preparation.
[26] R.S. MacKay and I.C. Percival, Self-similarity of the boundary of Siegel disks for arbitrary rotation number, in preparation.
[27] J.D. Meiss, Transport Near the Onset of Stochasticity, preprint, IFS, University of Texas, Austin (1985).
[28] J.D. Hanson, J.R. Cary and J.D. Meiss, Algebraic decay in self-similar Markov chains, J. Stat. Phys. 39 (1985) 327–345.
[29] J.D. Farmer and I.I. Satija, Renormalization of the quasiperiodic transition to chaos for arbitrary winding numbers, Phys. Rev. A 31 (1985) 3520–3522.
[30] J.D. Farmer, I.I. Satija and D. Umberger, A Universal Strange Attractor Underlying the Quasiperiodic Transition to Chaos, preprint, CNLS, Los Alamos (1984).
[31] S. Ostlund and S. Kim, Renormalization of quasiperiodic mappings, Physica Scripta T9 (1985) 193–198.
[32] P. Cvitanovic, B. Shraiman and B. Soderberg, Scaling laws for mode lockings in circle maps, to appear in Physica Scripta.
[33] J.M. Greene and R.S. MacKay, An approximation to the critical commuting pair for breakup of noble tori, Phys. Lett. 107A (1985) 1–4.
[34] R.S. MacKay and I.C. Percival, Converse KAM: theory and practice, Commun. Math. Phys. 98 (1985) 469–512.